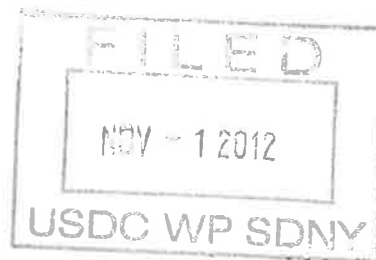


Francisco A. Villegas
fvillegas@cohengresser.com
Joyce E. Kung
jkung@cohengresser.com
COHEN & GRESSER LLP
800 Third Avenue, 21st Floor
New York, New York 10022
Telephone: (212) 957-7600
Facsimile: (212) 957-4514
Attorneys for Plaintiffs



12 CV 8023

**UNITED STATES DISTRICT COURT
FOR THE SOUTHERN DISTRICT OF NEW YORK**

NEUROGRAFIX; NEUROGRAPHY
INSTITUTE MEDICAL ASSOCIATES,
INC.; and IMAGE-BASED
SURGICENTER CORPORATION,

Plaintiffs,

vs.

THE TRUSTEES OF COLUMBIA
UNIVERSITY IN THE CITY OF NEW
YORK,

Defendant.

Civil Action No. _____

JURY TRIAL DEMANDED

**COMPLAINT FOR PATENT
INFRINGEMENT AND DEMAND FOR JURY TRIAL**

Plaintiffs NeuroGrafix, Neurography Institute Medical Associates, Inc. ("NIMA"), and Image-Based Surgicenter Corporation ("IBSC") (collectively, "Plaintiffs") allege as follows:

1. This case is an action for patent infringement of United States Patent No. 5,560,360 (the "'360 Patent") under the Patent Laws of the United States, as set forth in 35 U.S.C. §§271 and 280 through 285.

PARTIES

2. Plaintiff NIMA is incorporated in the State of Pennsylvania (Corporation # 3191217) and in the State of California (Corporation # 2127979) with its two principal places of business at 203 East 60th Street, New York, New York, 10022 (formerly at 75 Park Place New York, New York, 10007) and in Pasadena, California. Its designated representative and medical director, Dr. Aaron Filler, M.D., Ph.D. is a physician licensed in the State of New York (New York License # - 254556) and in the State of California (California License # - G81778). Dr. Filler practices medicine in California and in New York.

3. Plaintiff NeuroGrafix is a California corporation with its two principal places of business in Philadelphia, Pennsylvania (neurography marketing and neurography clinical technology) and in Santa Monica, California (corporate management & DTI research).

4. Plaintiff Image-Based Surgicenter Corporation ("IBSC") is a California corporation with its principal place of business in Santa Monica, California.

5. On information and belief, defendant The Trustees of Columbia University in the City of New York ("Columbia") is a New York non-profit educational corporation with its principal place of business located at 535 West 116th Street, New York, New York, 10027.

JURISDICTION AND VENUE

6. This Court has federal subject matter jurisdiction over this action under 28 U.S.C. §§1331, 1332(a)(1), 1332(c)(1) and 1338(a).

7. Venue is proper in this Court pursuant to 28 U.S.C. §§1391(a), 1391(c), and 1400(b), including without limitation because Defendant is advertising, marketing, using, selling, and/or offering to sell products in this Judicial District.

BACKGROUND

8. The University of Washington, a public institution of higher education in the state of Washington, is the owner by assignment of the '360 Patent entitled "Image Neurography and Diffusion Anisotropy Imaging." The '360 Patent issued on October 1, 1999. A true and correct copy of the '360 Patent is attached as Exhibit A.

9. Aaron G. Filler, Jay S. Tsuruda, Todd L. Richards, and Franklyn A. Howe are listed as the inventors of the '360 Patent.

10. Washington Research Foundation ("WRF"), a not-for-profit corporation incorporated and existing under the laws of the State of Washington, holds substantially all rights in the '360 Patent and has exclusively licensed substantially all rights in the '360 Patent to NeuroGrafix in December of 1998. On June 15, 2012, WRF and NeuroGrafix entered into an Amended and Restated Non-Terminable Exclusive License Agreement in which WRF granted NeuroGrafix an exclusive license to substantially all rights in the '360 Patent and retained no reversionary rights to the '360 Patent.

11. On September 14, 2011, NeuroGrafix and NIMA entered into an amended license agreement in which NIMA received the exclusive right to practice the '360 Patent in all fields of use, but granted back to NeuroGrafix an exclusive license to practice the '360 Patent in the field of use of non-human, non-surgical medicine. On September 14, 2011, NIMA and IBSC entered into an exclusive license agreement in which NIMA granted to IBSC an exclusive license to practice the '360 Patent in the field of human, surgical medicine. Accordingly, NeuroGrafix has an exclusive license to the '360 Patent in the field of use of non-human, non-surgical medicine, IBSC has an exclusive license in the field of use of human, surgical medicine, and NIMA has an exclusive license in the field of use of human, nonsurgical medicine.

12. NeuroGrafix, NIMA and IBSC have been investing in and practicing the technology disclosed in the '360 Patent since at least 2000.

COUNT I
PATENT INFRINGEMENT

13. Plaintiffs repeat and reallege the allegations contained in paragraphs 1 through 12 above, inclusive, as if fully repeated and restated herein.

14. Defendant has been and still is directly (literally and under the doctrine of equivalents) infringing at least claim 36 of the '360 Patent by making, using, selling, offering to sell, or importing, without license or authority, products and services that include, without limitation, the performance of diffusion tensor imaging and diffusion anisotropy based tractography. Thus, by making, using, importing, offering for sale, and/or selling such products and software, Defendant has injured Plaintiffs and are thus liable to Plaintiffs for infringement of the '360 Patent under 35 U.S.C. § 271(a).

15. To the extent that facts learned in discovery show that Defendant's infringement of the '360 Patent is or has been willful, Plaintiffs reserve the right to request such a finding at the time of trial.

16. As a result of Defendant's infringement of the '360 Patent, Plaintiffs have suffered monetary damages in an amount not yet determined, and will continue to suffer damages in the future unless Defendant's infringing activities are enjoined by this Court.

17. Defendant's wrongful acts have damaged and will continue to damage Plaintiffs irreparably, and Plaintiffs have no adequate remedy at law for those wrongs and injuries. In addition to their actual damages, Plaintiffs are entitled to a preliminary and permanent injunction restraining and enjoining Defendant and its agents, servants and employees, and all persons acting thereunder, in concert with, or on its behalf, from infringing the '360 Patent.

PRAYER FOR RELIEF

WHEREFORE, Plaintiffs respectfully request that this Court enter:

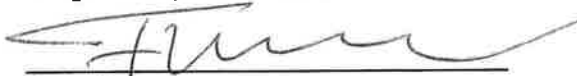
1. A judgment in favor of Plaintiffs that Defendant has directly infringed the '360 Patent;
2. An injunction enjoining Defendant and its officers, directors, agents, servants, affiliates, employees, divisions, branches, subsidiaries, parents, and all others acting in concert or privity with any of them from infringing the '360 Patent;
3. A judgment and order requiring Defendant to pay Plaintiffs their damages, costs, expenses, and prejudgment and post-judgment interest for Defendant's infringement of the '360 Patent as provided under 35 U.S.C. § 284;
4. A judgment and order finding that this is an exceptional case within the meaning of 35 U.S.C. § 285 and awarding to Plaintiffs their reasonable attorneys' fees; and
5. Any and all other relief to which Plaintiffs may show themselves to be entitled.

JURY TRIAL DEMANDED

Plaintiffs hereby demand a trial by jury of all issues so triable.

Dated: November 1, 2012

Respectfully submitted,



Francisco A. Villegas

fvillegas@cohengresser.com

Joyce E. Kung

jkung@cohengresser.com

COHEN & GRESSER LLP

800 Third Avenue, 21st Floor

New York, NY 10022

Telephone: (212) 957-7600

Facsimile: (212) 957-4514

Of Counsel:

Marc A. Fenster

mfenster@raklaw.com

Andrew D. Weiss

aweiss@raklaw.com

Fredricka Ung

fung@raklaw.com

Russ August & Kabat

12424 Wilshire Boulevard, 12th Floor

Los Angeles, CA 90025

Telephone: (310) 826-7474

Facsimile: (310) 826-6991

*Attorneys for Plaintiffs Neurography Institute
Medical Associates, Inc., NeuroGrafix, and Image-
Based Surgicenter Corporation*

EXHIBIT A



US005560360A

United States Patent [19]

Filler et al.

[11] **Patent Number:** **5,560,360**[45] **Date of Patent:** **Oct. 1, 1996**[54] **IMAGE NEUROGRAPHY AND DIFFUSION ANISOTROPY IMAGING**[75] **Inventors:** **Aaron G. Filler**, Seattle; **Jay S. Tsurda**, Mercer Island; **Todd L. Richards**, Seattle, all of Wash.; **Franklyn A. Howe**, London, England[73] **Assignee:** **University of Washington**, Seattle, Wash.[21] **Appl. No.:** **28,795**[22] **Filed:** **Mar. 8, 1993**[30] **Foreign Application Priority Data**

Mar. 9, 1992	[GB]	United Kingdom	9205058
Mar. 13, 1992	[GB]	United Kingdom	9205541
Mar. 30, 1992	[GB]	United Kingdom	9207013
May 5, 1992	[GB]	United Kingdom	9209648
May 21, 1992	[GB]	United Kingdom	9210810
Jul. 31, 1992	[GB]	United Kingdom	9216383
Jan. 22, 1993	[GB]	United Kingdom	9301268

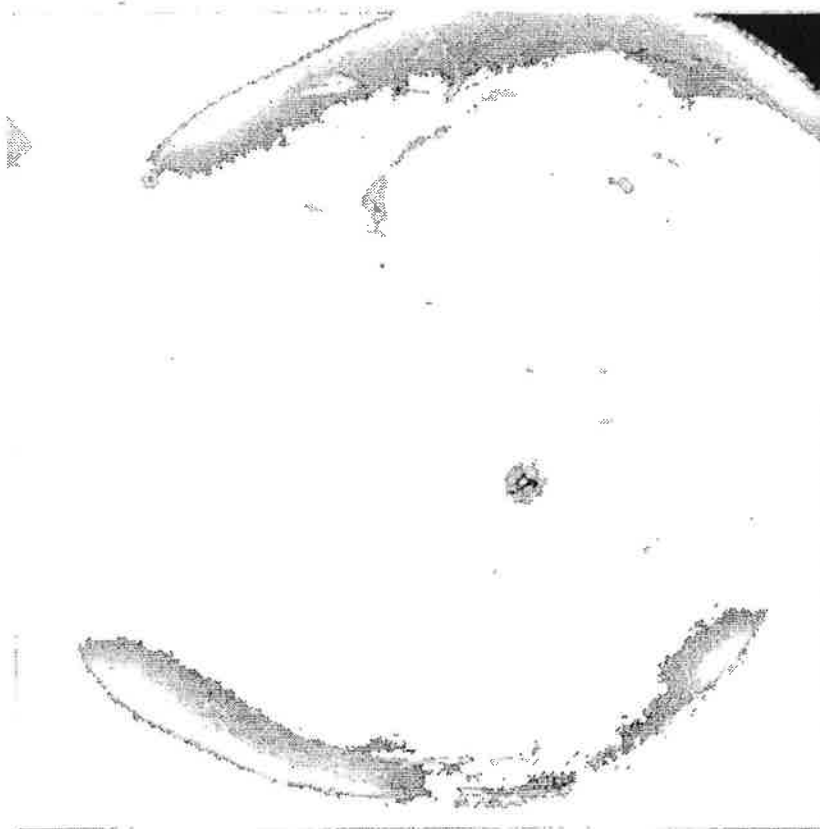
[51] **Int. Cl.⁶** **A61B 5/055**[52] **U.S. Cl.** **128/653.2; 324/307**[58] **Field of Search** **128/653.1, 653.2, 128/653.3; 324/307, 309**[56] **References Cited****U.S. PATENT DOCUMENTS**

3,735,247 5/1973 Harker 128/653.1

4,902,973	2/1990	Keren	324/312
5,070,876	12/1991	Wright	128/653.3
5,078,141	1/1992	Suzuki et al.	324/309
5,079,505	1/1992	Deimling et al.	324/309
5,134,372	7/1992	Inoue	324/309
5,151,655	9/1992	Harms et al.	324/309
5,218,964	6/1993	Sepponen	324/309
5,250,899	10/1993	Listerud et al.	324/309
5,261,405	11/1993	Fossel	128/653.2

Primary Examiner—Marvin M. Lateef*Assistant Examiner*—Brian L. Casler*Attorney, Agent, or Firm*—Christensen, O'Connor, Johnson & Kindness PLLC[57] **ABSTRACT**

A neurography system (10) is disclosed for generating diagnostically useful images of neural tissue (i.e., neurograms) employing a modified magnetic resonance imaging system (14). In one embodiment, the neurography system selectively images neural tissue by employing one or more gradients to discriminate diffusion anisotropy in the tissue and further enhances the image by suppressing the contribution of fat to the image. The neurography system is part of a broader medical system (12), which may include an auxiliary data collection system (22), diagnostic system (24), therapeutic system (26), surgical system (28), and training system (30). These various systems are all constructed to take advantage of the information provided by the neurography system regarding neural networks, which information was heretofore unavailable.

66 Claims, 17 Drawing Sheets

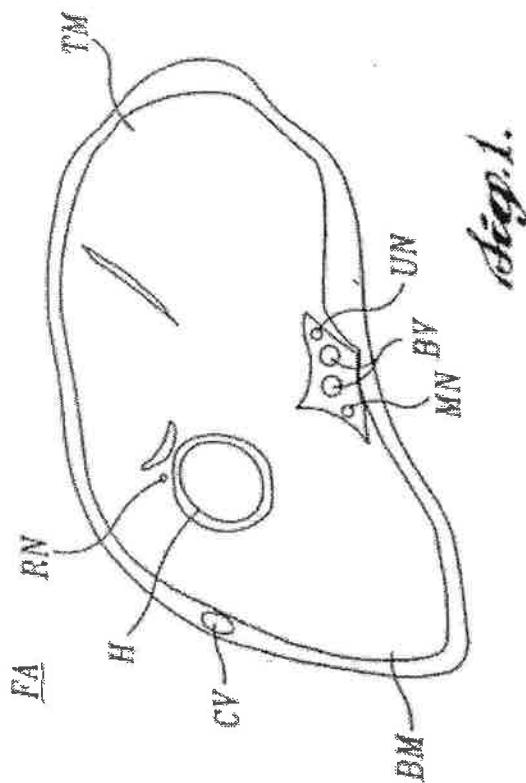


Fig. 1.

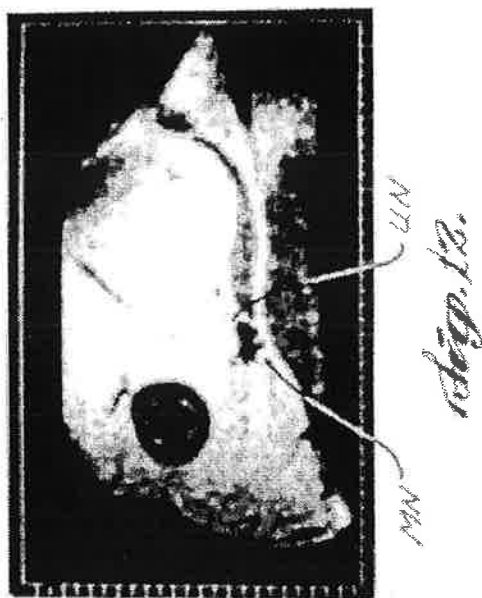


Fig. 13.

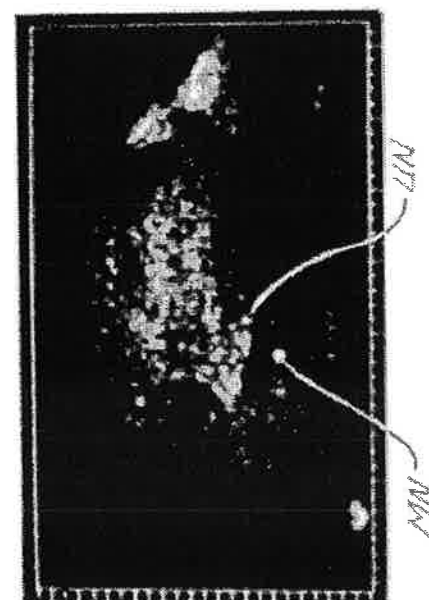


Fig. 13.A.

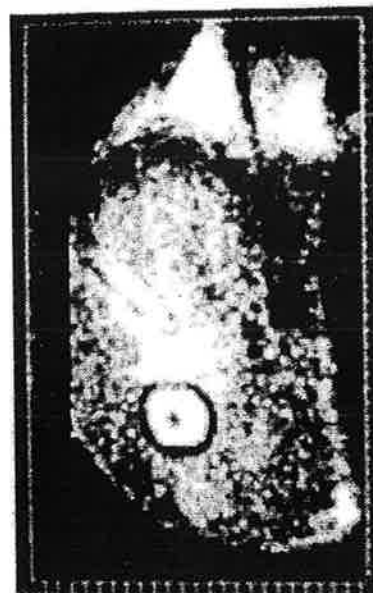


Fig. 13.B.

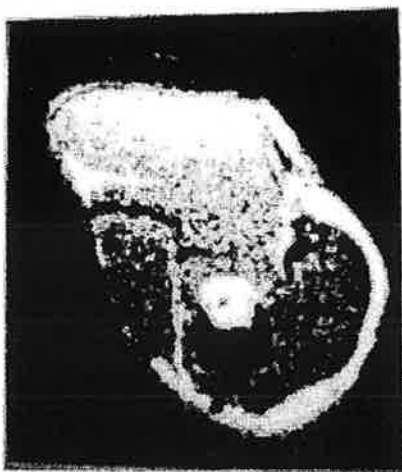


Fig. 2B.



Fig. 5B.

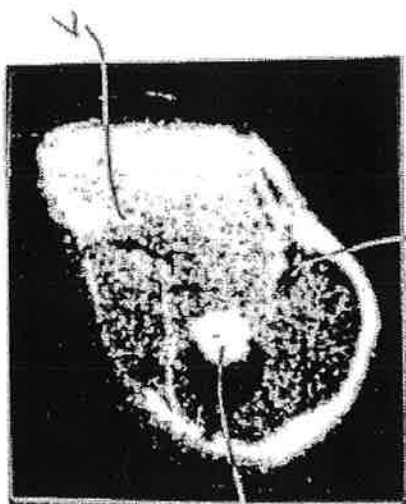


Fig. 2A.



Fig. 5A.

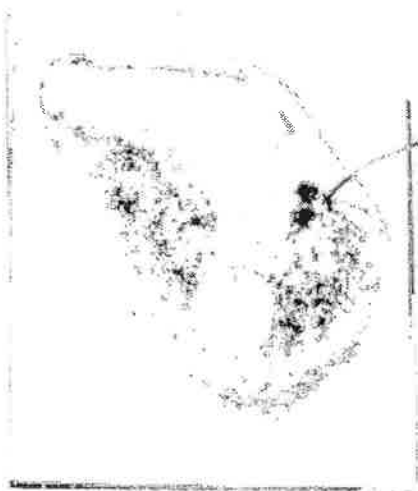


Fig. 3.



Fig. 4.

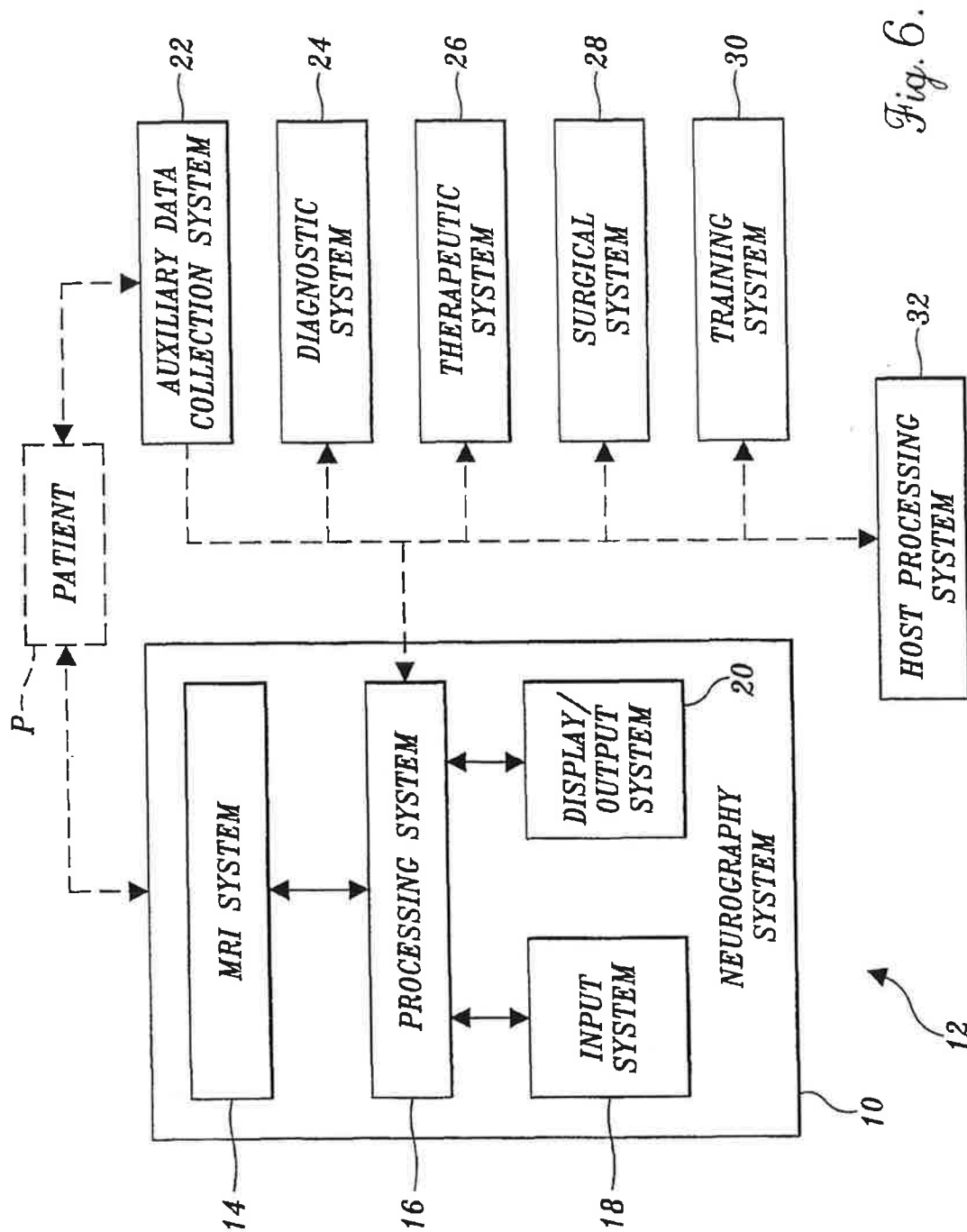


Fig. 6.

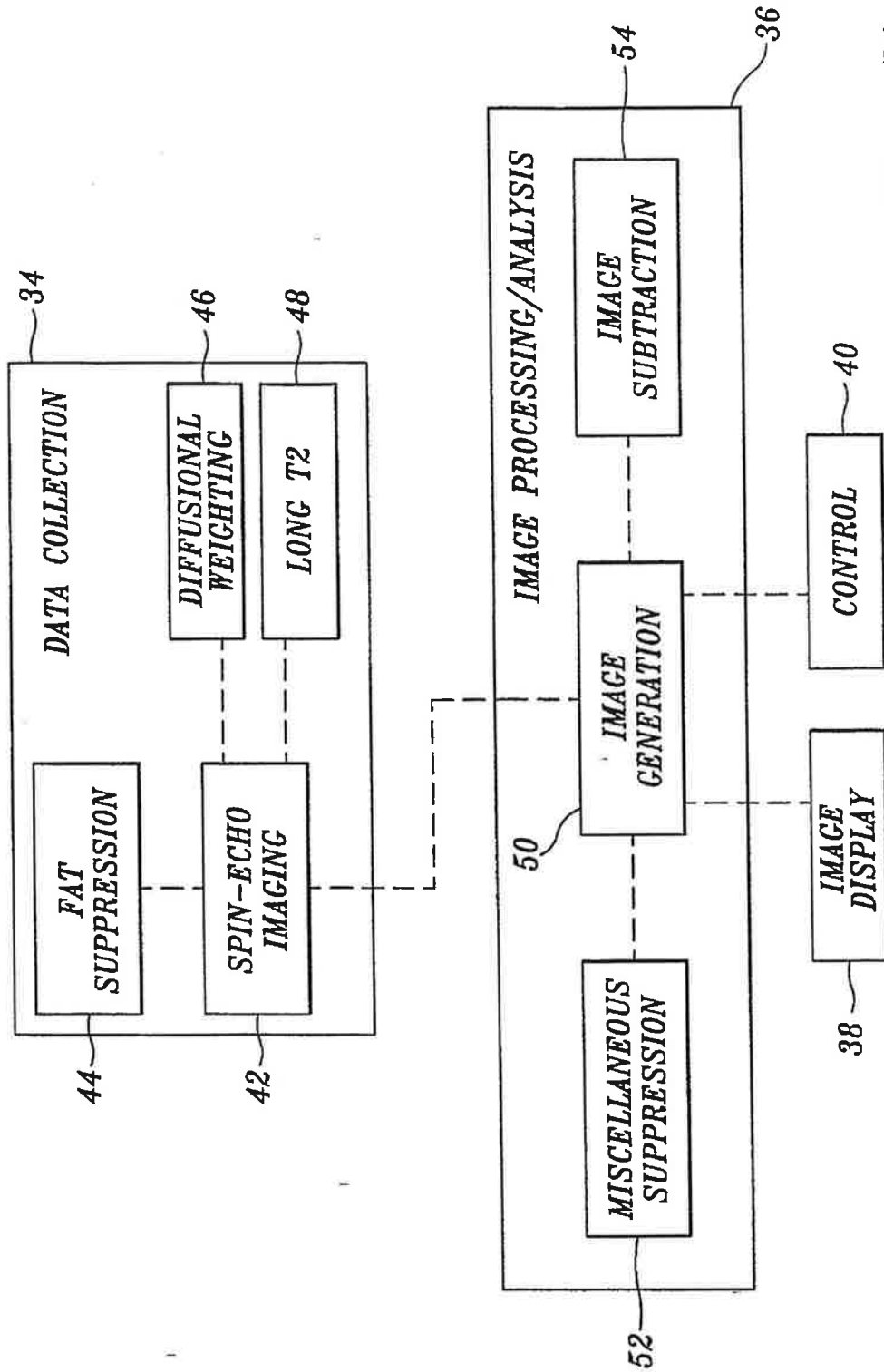
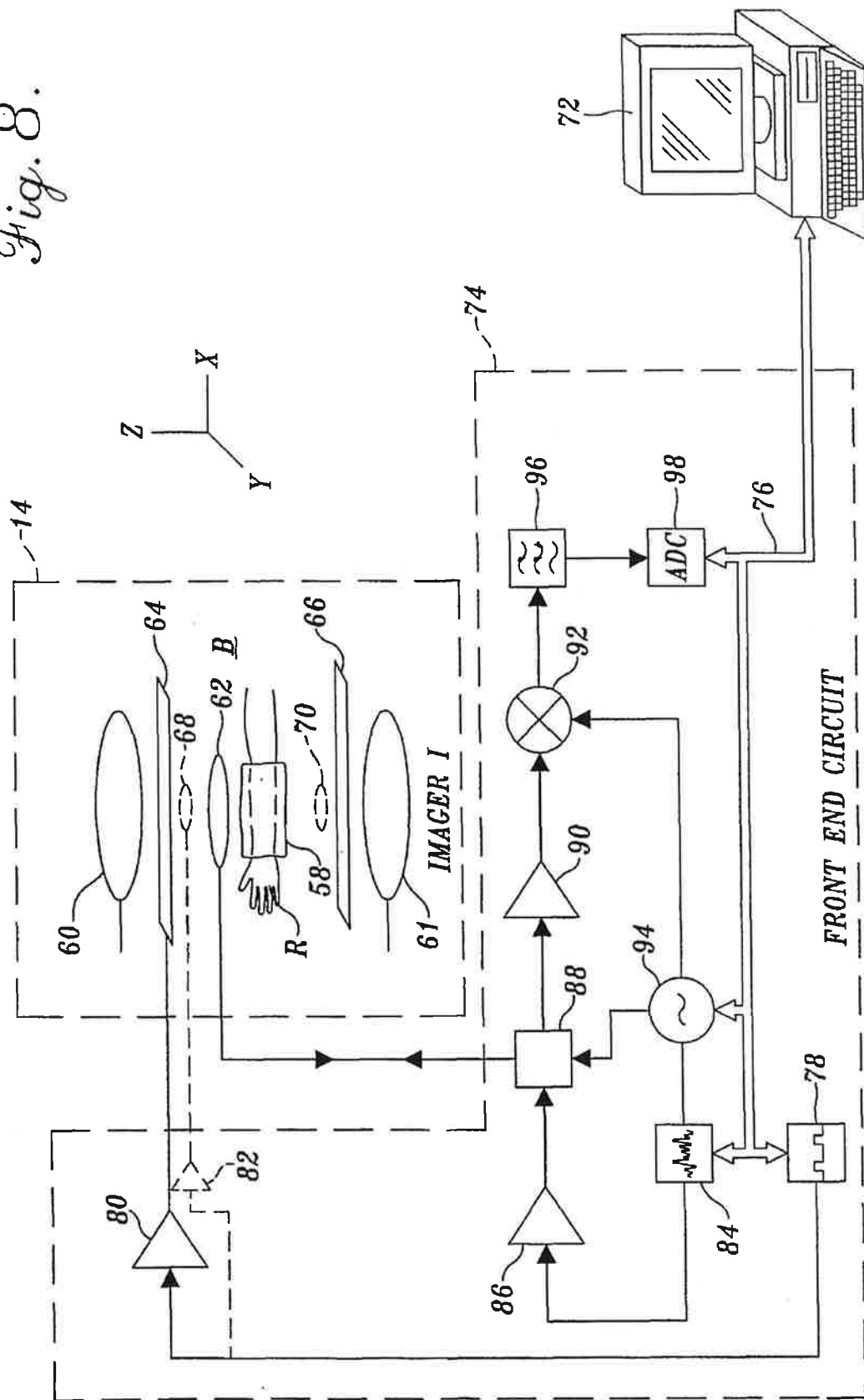
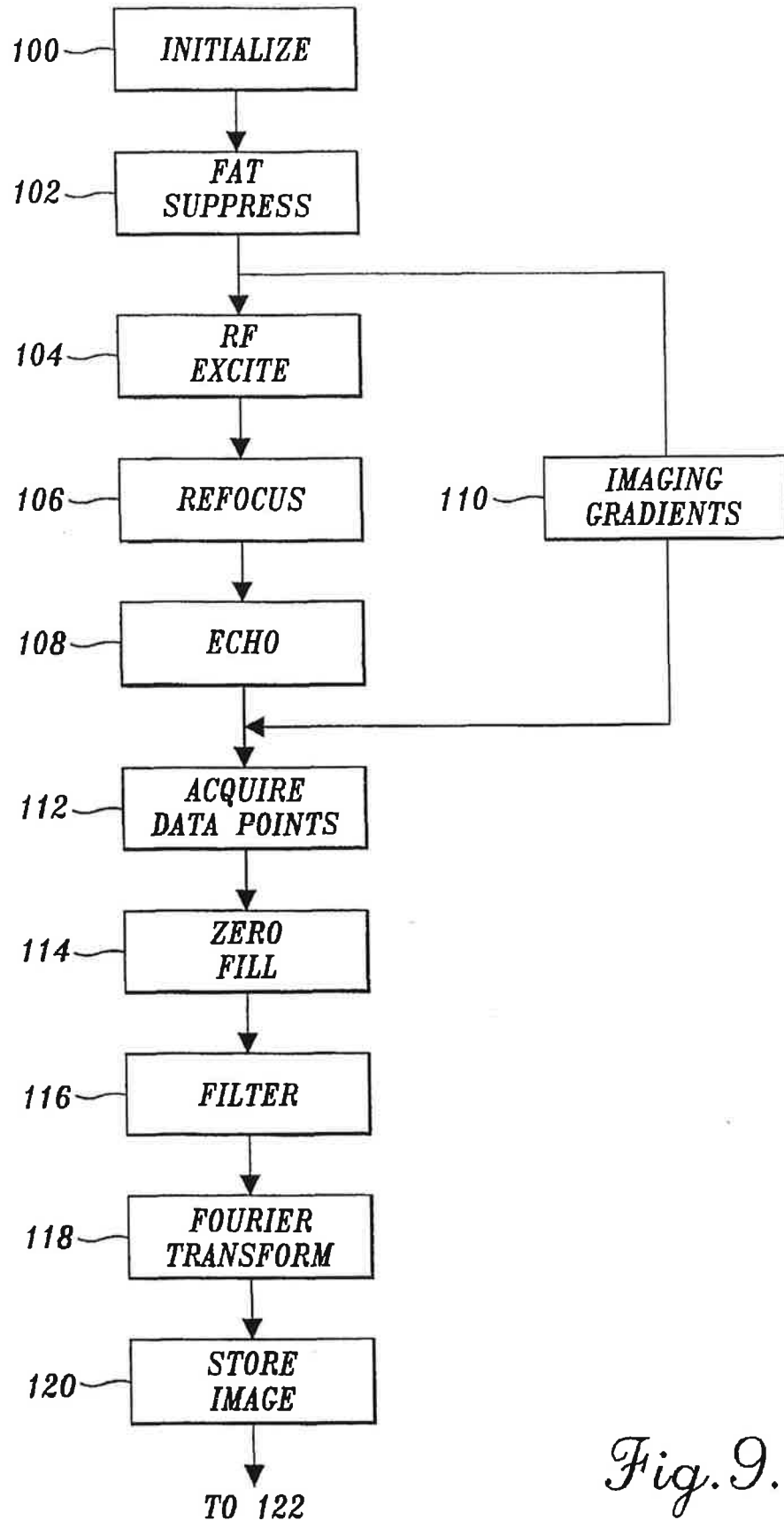
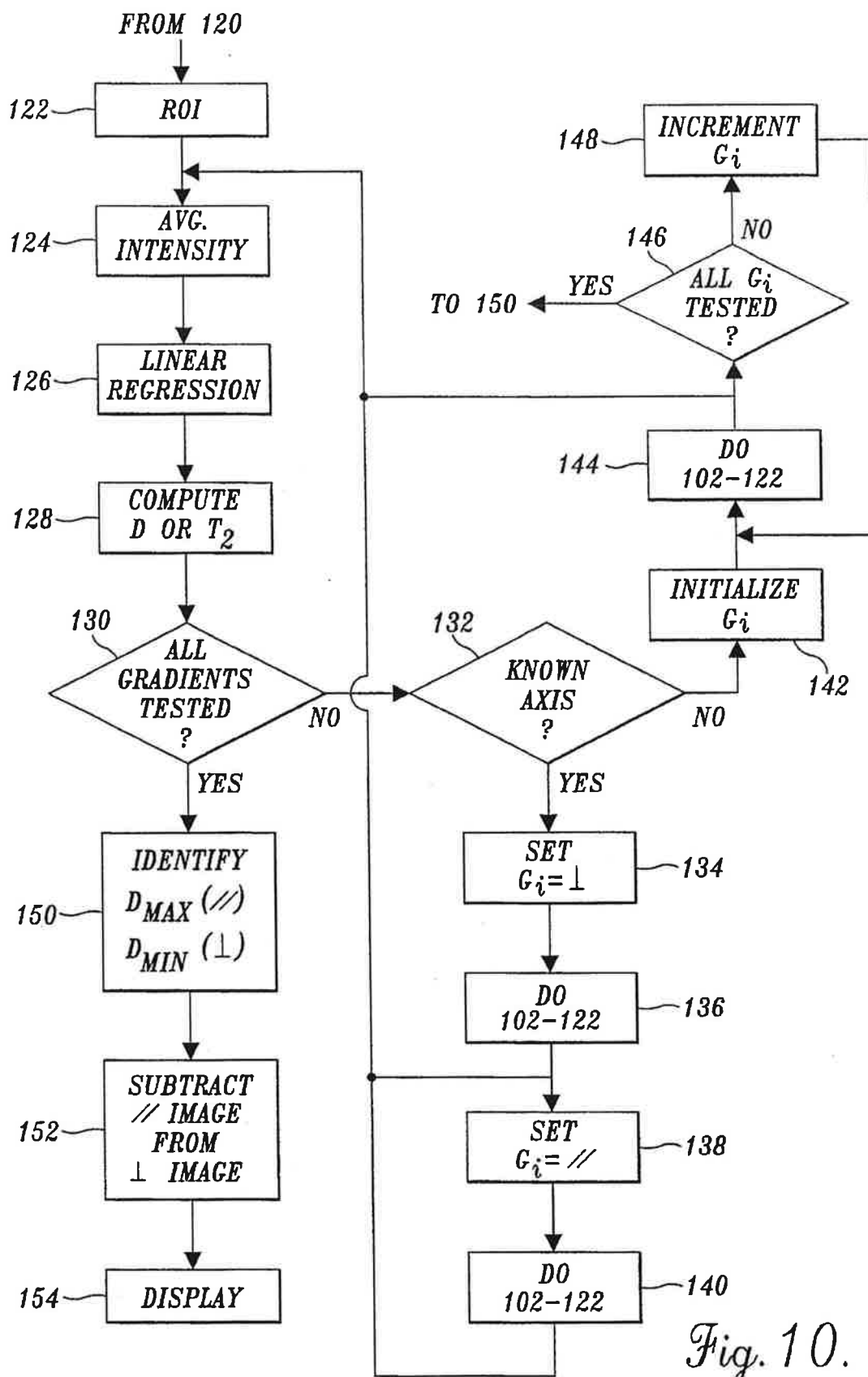


Fig. 7.

Fig. 8.



*Fig. 9.*



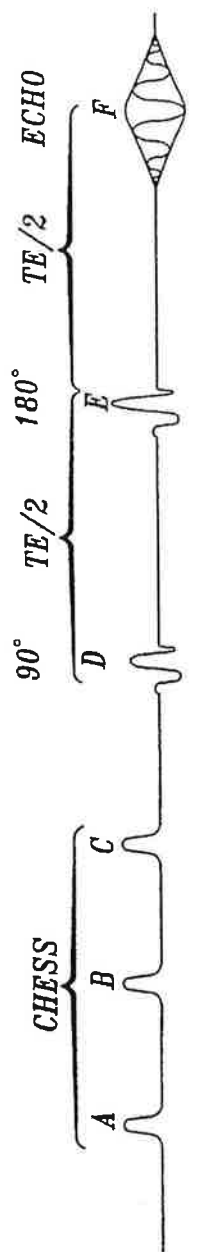


Fig. 11A. RADIO FREQUENCY PULSES



Fig. 11B. DEPHASING/ SPOILER GRADIENTS



Fig. 11C. SLICE SELECTION GRADIENTS



Fig. 11D. FREQUENCY ENCODING/ READOUT GRADIENT

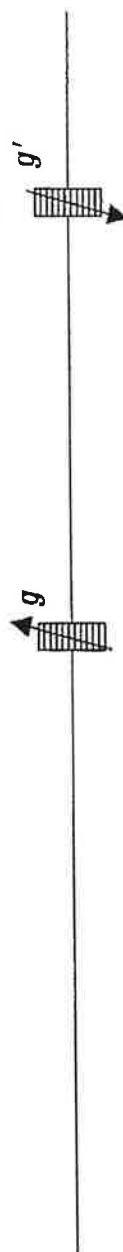


Fig. 11E. PHASE ENCODING

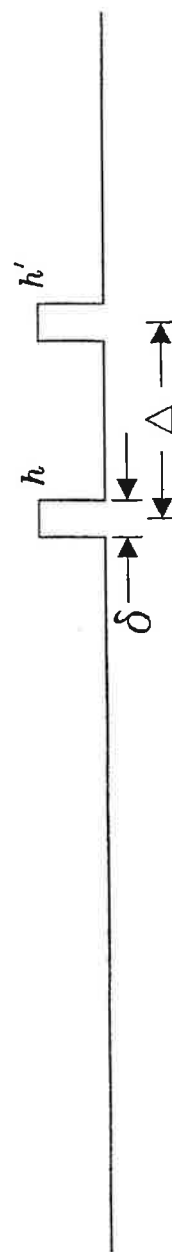


Fig. 11F. DIFFUSION SENSITIZING GRADIENTS

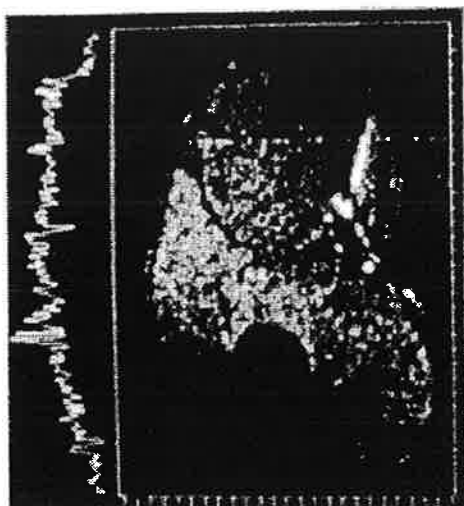


Fig. 14B.

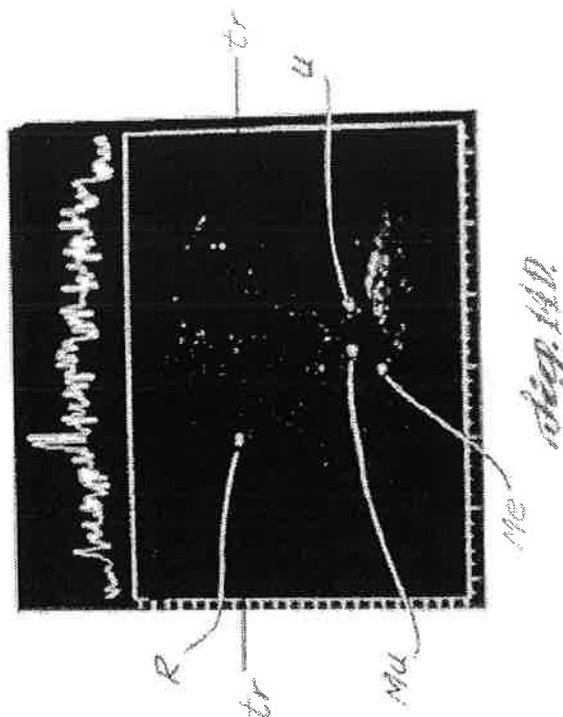


Fig. 14D.

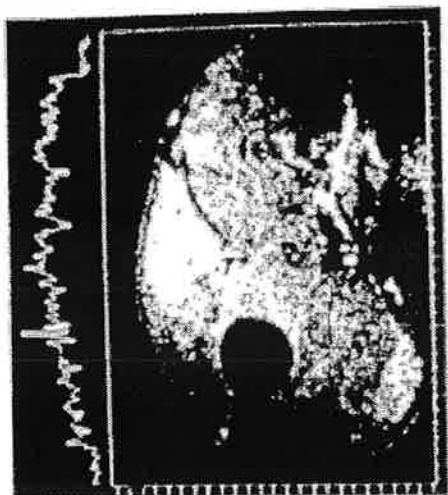


Fig. 14A.

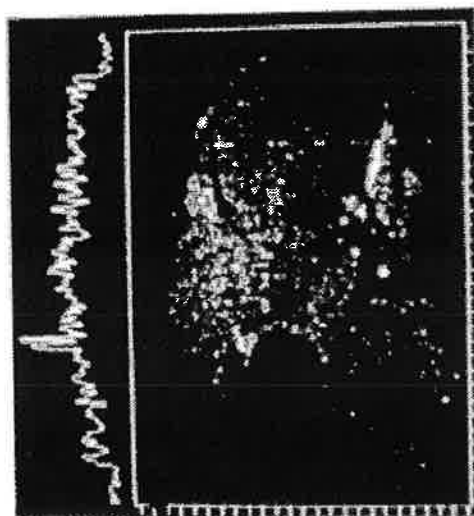


Fig. 14C.

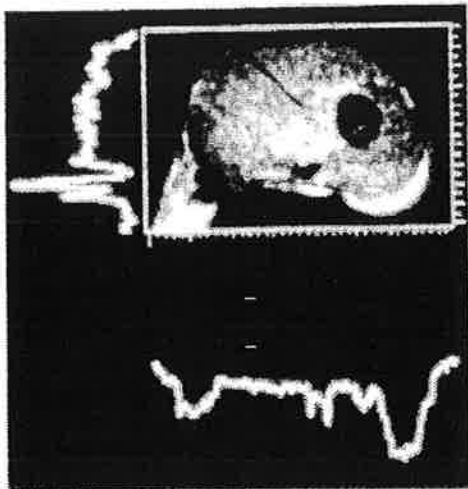


Fig. 15B.

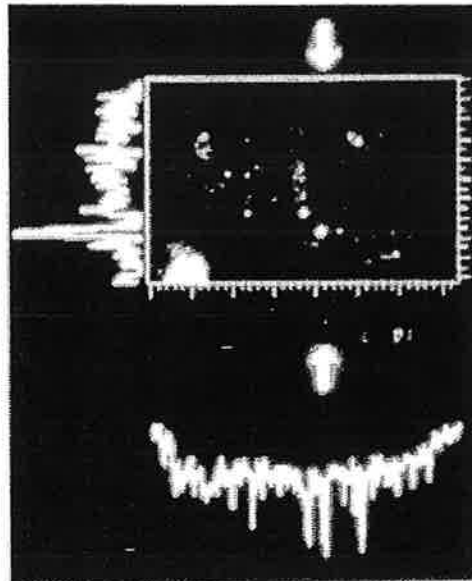


Fig. 15C.

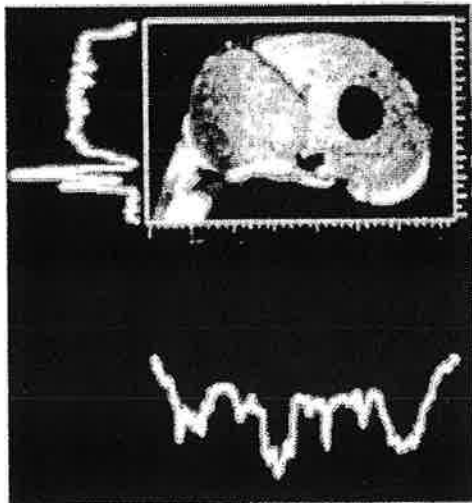


Fig. 15D.

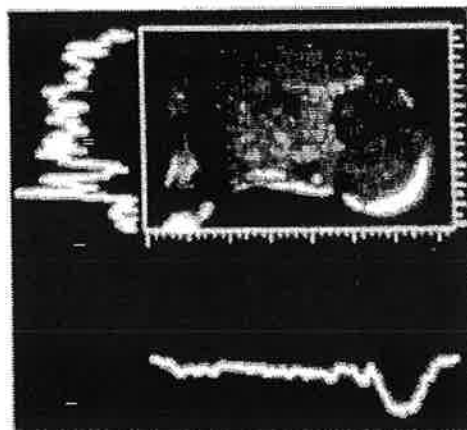


Fig. 15E.



Fig. 16.

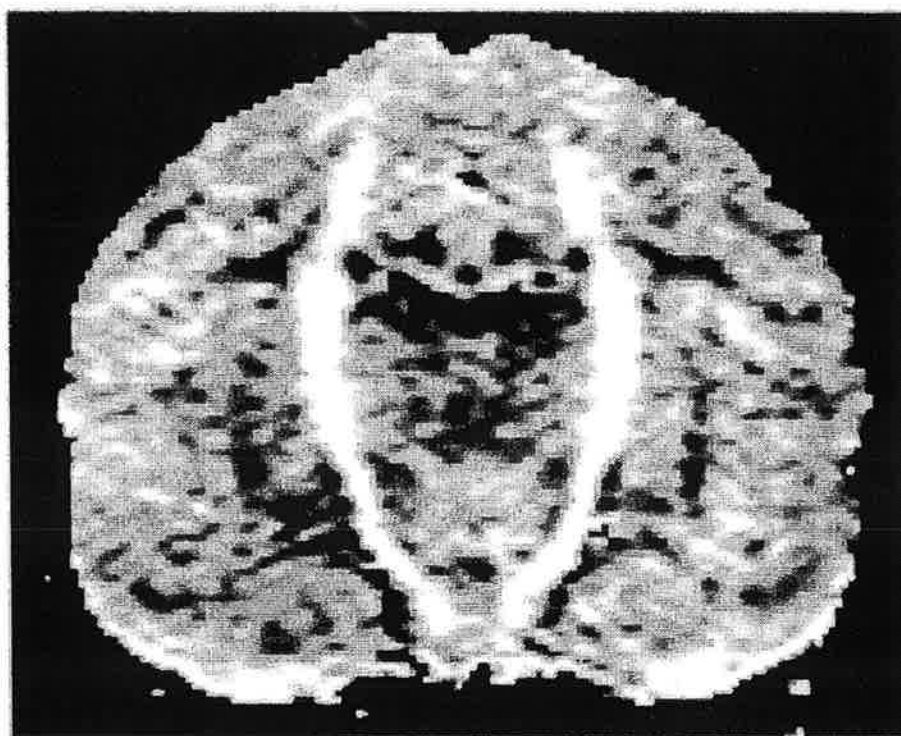


Fig. 17.



Fig. 18B

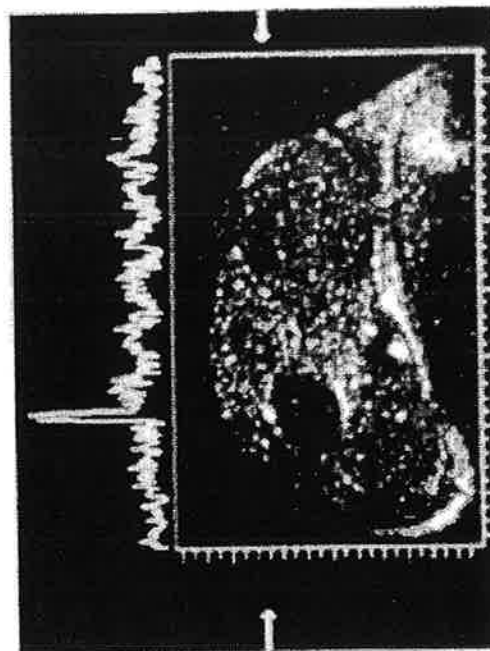


Fig. 18D

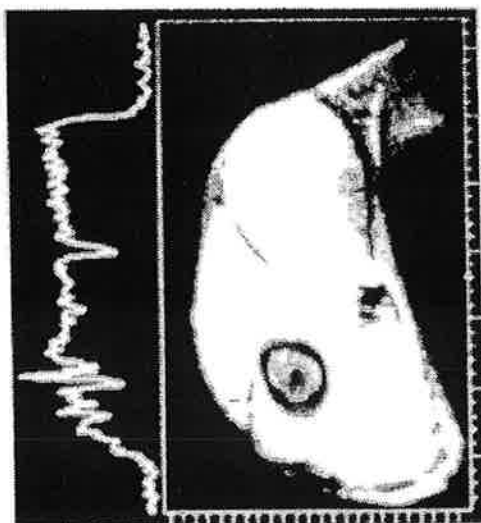


Fig. 18A

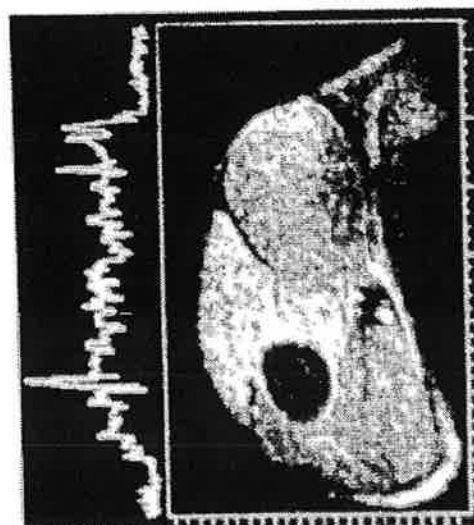
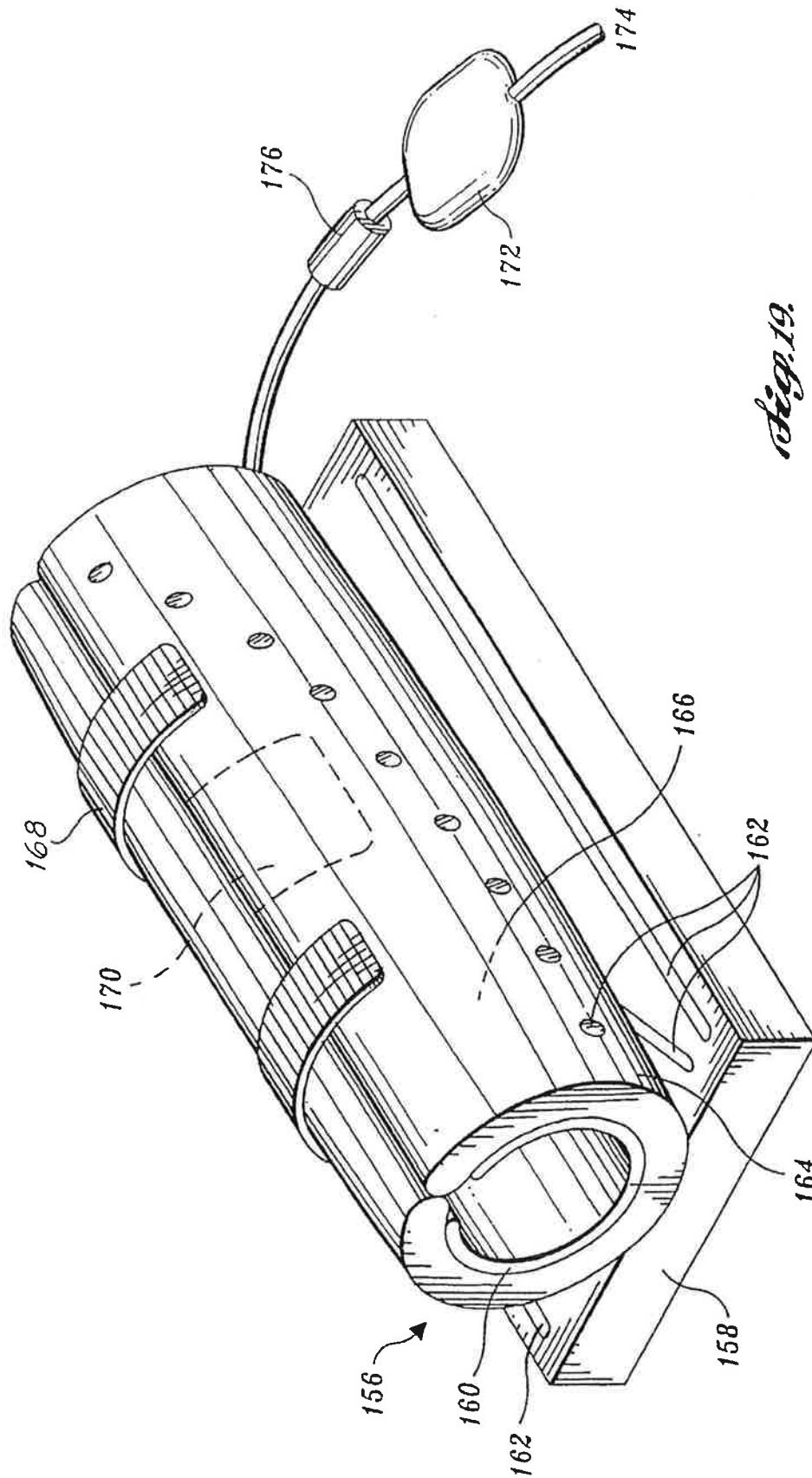


Fig. 18C



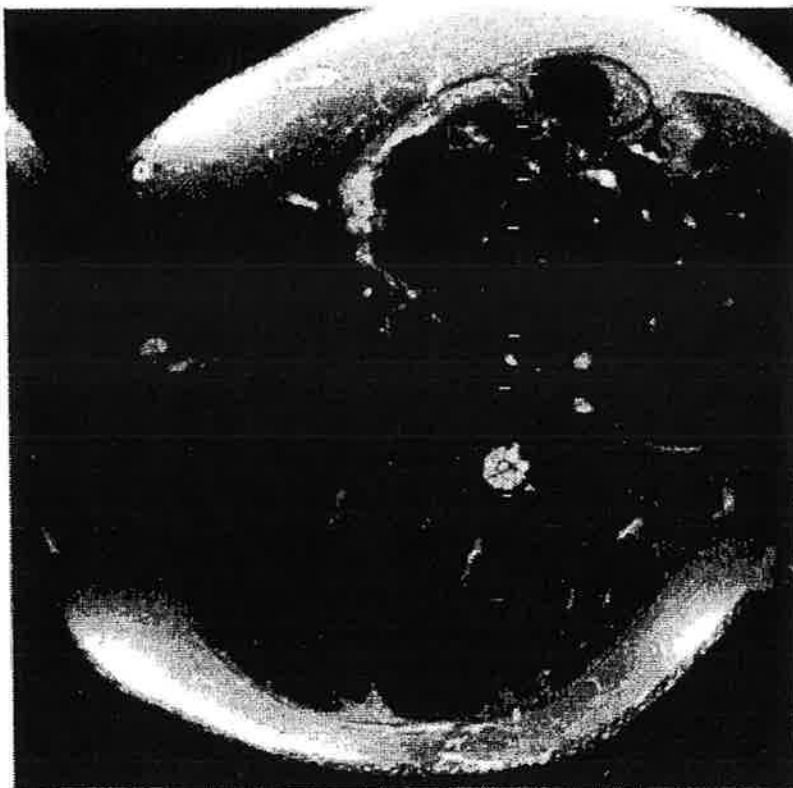


Fig. 20.

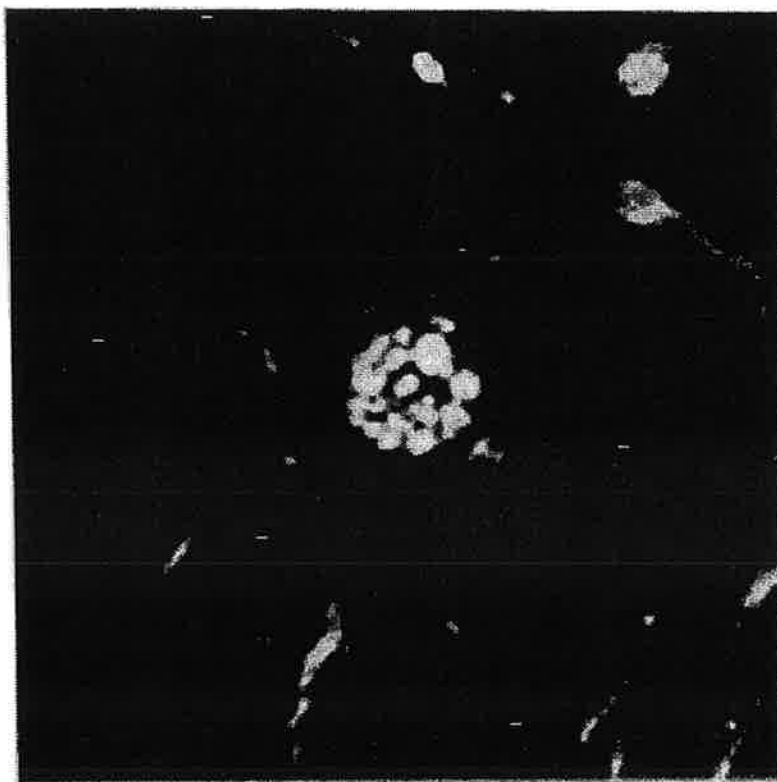


Fig. 21.

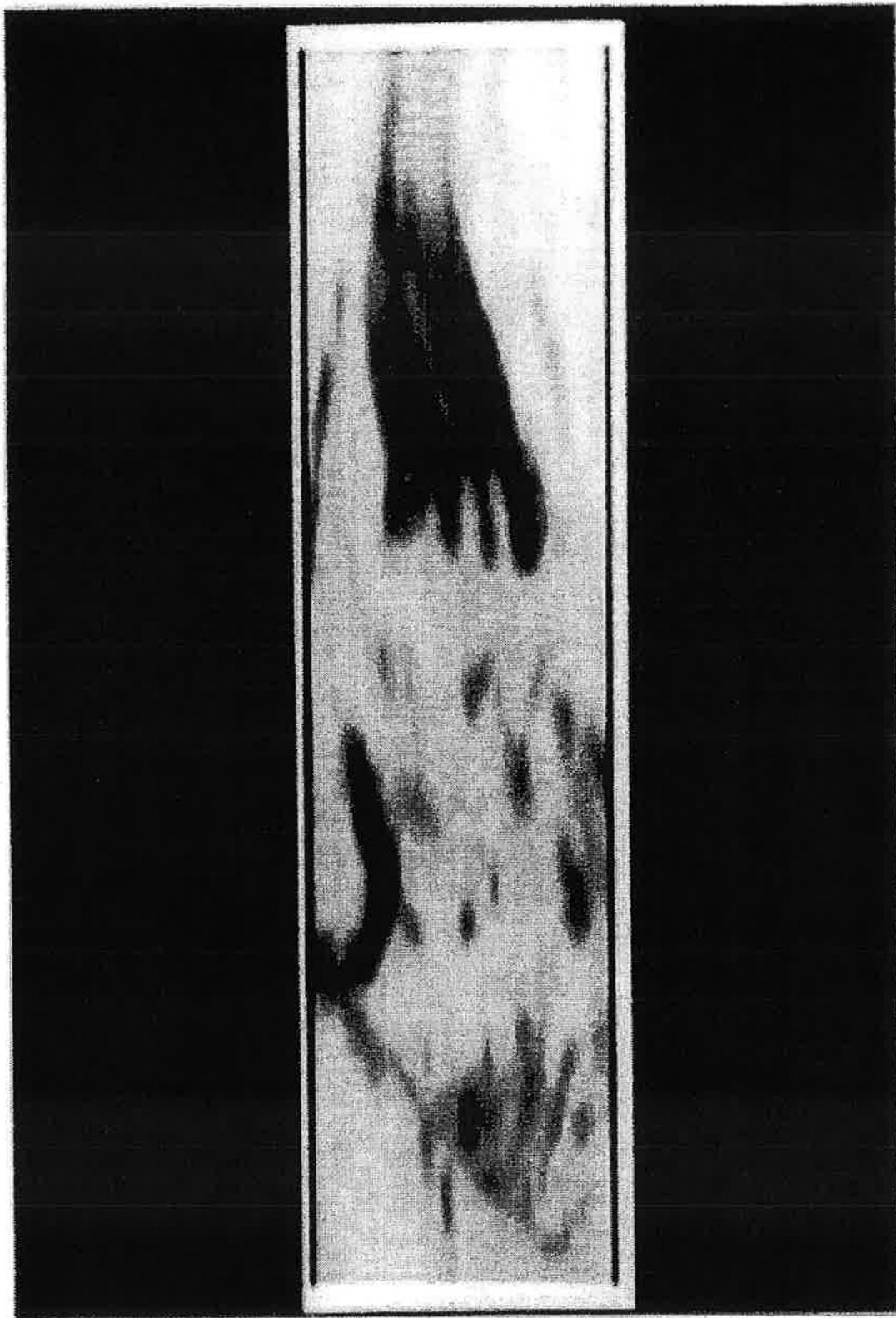
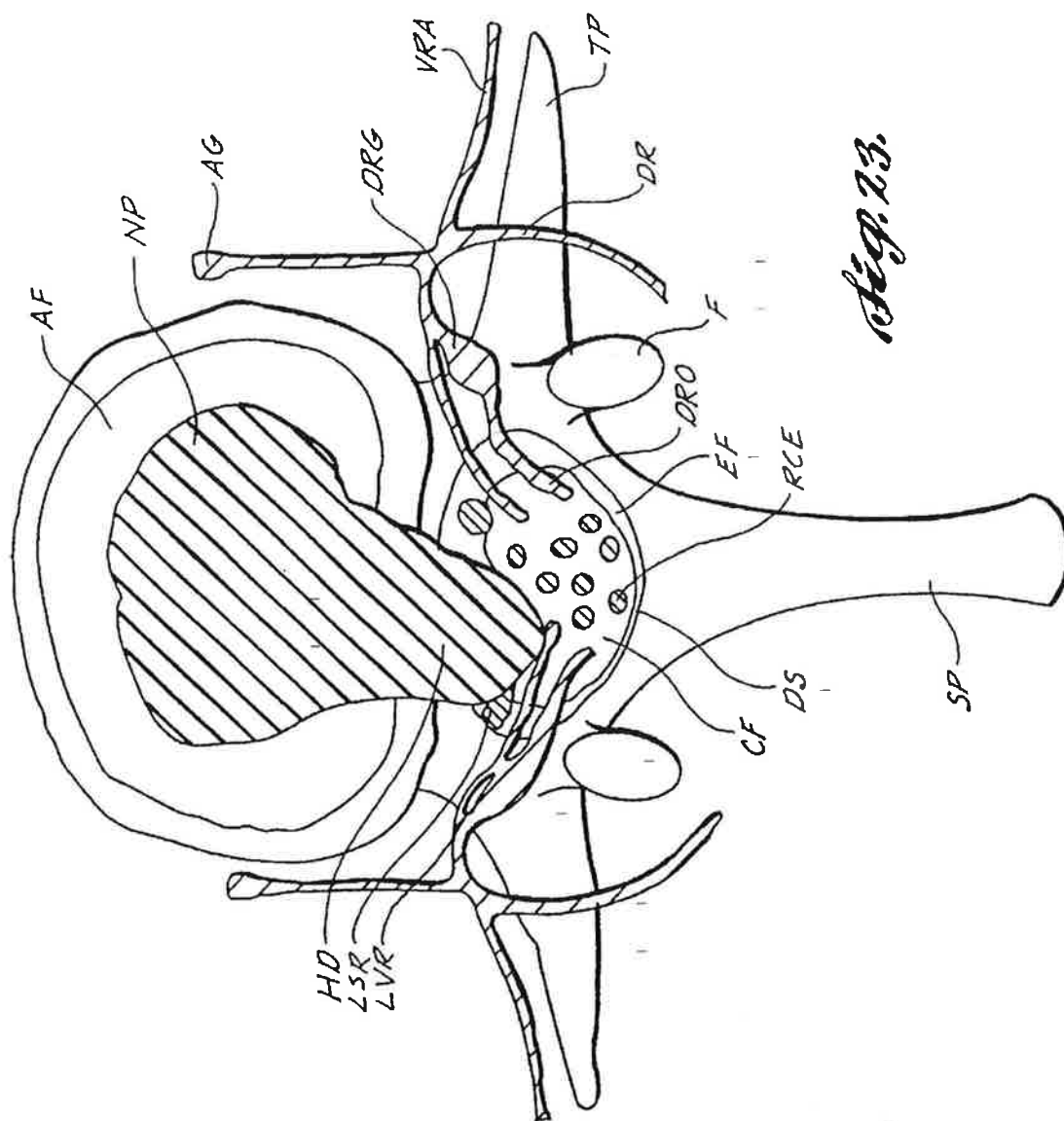


Fig. 22.



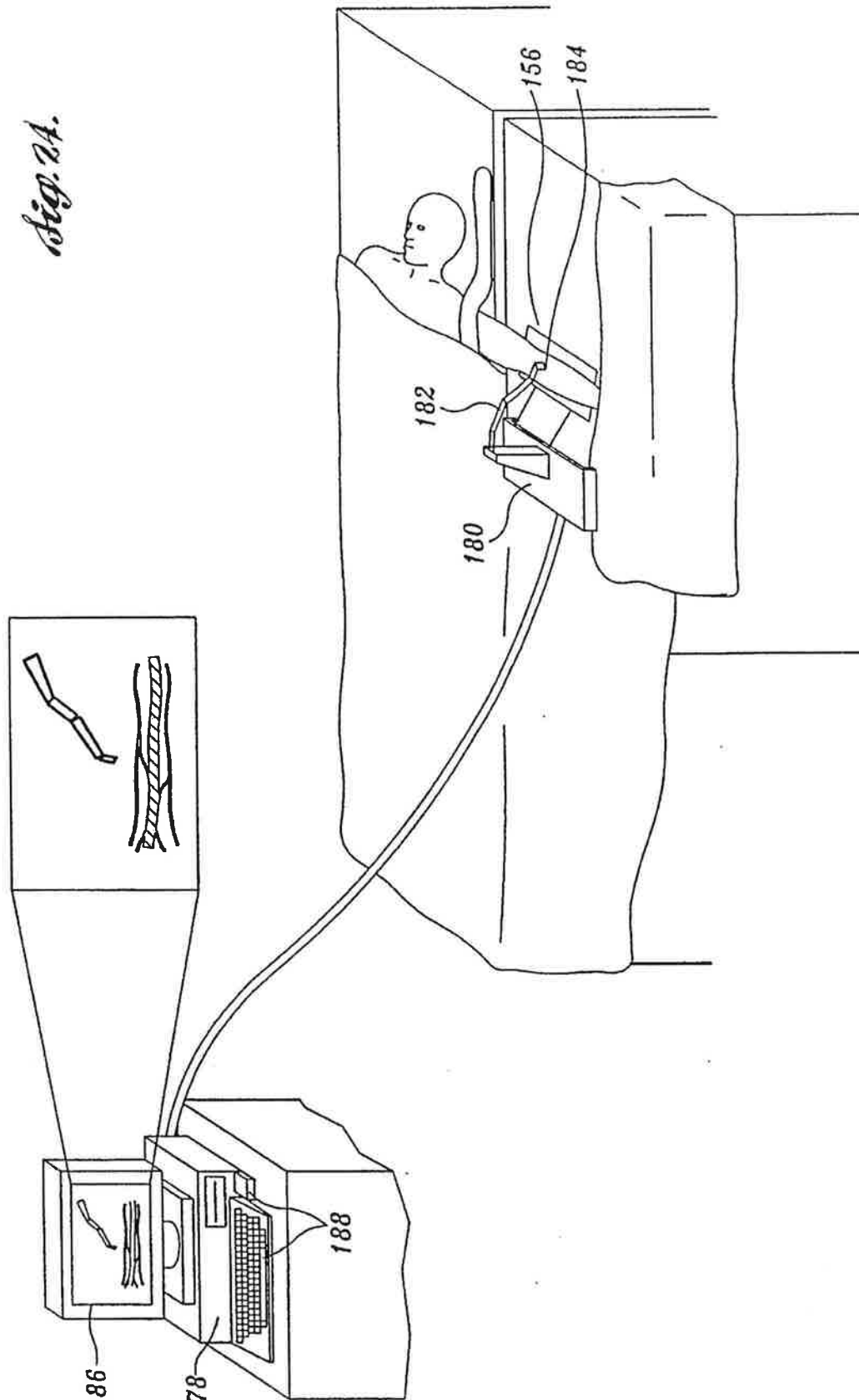


IMAGE NEUROGRAPHY AND DIFFUSION ANISOTROPY IMAGING

This application is based upon an earlier filed U.K. Patent Application No. 9301268.0, filed Jan. 22, 1993, which, in turn, is a continuation-in-part of U.K. Patent Application No. 9216383.1, filed Jul. 31, 1992, which, in turn, is a continuation-in-part of U.K. Patent Application No. 9210810.9, filed May 21, 1992, which, in turn, is a continuation-in-part of U.K. Patent Application No. 9209648.6, filed May 5, 1992, which, in turn, is a continuation-in-part of U.K. Patent Application No. 9207013.5, filed Mar. 30, 1992, which, in turn, is a continuation-in-part of U.K. Patent Application No. 9205541.7, filed Mar. 13, 1992, which, in turn, is a continuation-in-part of parent U.K. Patent Application No. 9205058.2, filed Mar. 9, 1992, the benefit of the filing dates of which is hereby claimed pursuant to 35 U.S.C. §119.

FIELD OF THE INVENTION

The present invention relates generally to the field of imaging and, more particularly, to the imaging of nerve tissue and other diffusionally anisotropic structures.

BACKGROUND OF THE INVENTION

Although many techniques have been developed for locating and viewing the brain, spinal cord, and spinal roots within the spinal canal, hitherto there has not been a successful method for viewing the peripheral, autonomic, and cranial nerves. These nerves, collectively referred to herein as peripheral nerves, commonly travel through and along bone, muscle, lymphatics, tendons, ligaments, intermuscular septa, collections of fatty tissues, air and fluid spaces, veins, arteries, joints, skin, mucous membranes and other tissues. The relatively small size of peripheral nerves, as well as their close proximity to other tissue of comparable size and shape, makes them difficult to locate and identify.

The examination of peripheral nerves is further complicated by the complexity of many such neural structures, such as the brachial plexus, lumbar plexus, and sacral plexus. These structures include bundles of nerves that may join together, separate, rejoin, intermix, and segregate, forming intricate three dimensional patterns. A compression or irritation of a small area of nerve within such a plexus (e.g. in the shoulder) can cause pain, numbness, weakness or paralysis at some distant site (e.g. in one finger). Even when a surgeon attempts to expose the plexus for direct inspection, the anatomic complexity can prove overwhelming, rendering diagnosis inconclusive and surgery difficult and dangerous.

Radiologic methods employing, for example, X-rays, have been developed to generate tissue specific images of various physiological structures including bone, blood vessels, lymphatics, the gastrointestinal tract, and the tissues of the central nervous system. Due in part to the neural characteristics noted above, however, these techniques have not been successfully used to generate suitable clinical images of peripheral nerves.

Typically, the position of peripheral nerves in radiologic images has been inferred by reference to more conspicuous, non-neural structures such as tendons, vessels, or bone. For example, by producing an X-ray image of a region of the body through which a nerve of interest passes, non-neural structures can often be readily identified. Then, the locations of peripheral nerves in the region can be inferred from standard reference information about human anatomy. Due

to the variability of nerve position from one individual to another, however, this technique is of limited value.

One approach of particular interest that has been used to image physiological structures is magnetic resonance imaging (MRI). By way of introduction, MRI involves the exposure of tissue to a variety of different magnetic and radio-frequency (rf) electromagnetic fields. The response of the specimen's atomic nuclei to the fields is then processed to produce an image of the specimen.

More particularly, the specimen is initially exposed to a polarizing magnetic field. In the presence of this field, nuclei exhibiting magnetic moments (hereinafter referred to as spins) will seek to align themselves with the field. The nuclei precess about the polarizing field at an angular frequency (hereinafter referred to as the Larmor frequency) whose magnitude depends upon both the field's strength and the magnetogyric constant of the specific nuclear species involved.

Although the magnetic components of the spins cancel each other in a plane perpendicular to the polarizing field, the spins exhibit a net magnetic moment in the direction of the polarizing field. By applying an excitation field perpendicular to the polarizing field and at a frequency near the Larmor frequency, the net magnetic moment can be tilted. The tilted magnetic moment includes a transverse component, in the plane perpendicular to the polarizing field, rotating at the Larmor frequency. The extent to which the magnetic moment is tilted and, hence, the magnitude of the net transverse magnetic moment, depends upon the magnitude and duration of the excitation field.

An external return coil is used to sense the field associated with the transverse magnetic moment, once the excitation field is removed. The return coil, thus, produces a sinusoidal output, whose frequency is the Larmor frequency and whose amplitude is proportional to that of the transverse magnetic moment. With the excitation field removed, the net magnetic moment gradually reorients itself with the polarizing field. As a result, the amplitude of the return coil output decays exponentially with time.

Two factors influencing the rate of decay are known as the spin-lattice relaxation coefficient T_1 and the spin-spin relaxation coefficient T_2 . The spin-spin relaxation coefficient T_2 represents the influence that interactions between spins have on decay, while the spin-lattice relaxation coefficient T_1 represents the influence that interactions between spins and fixed components have on decay. Thus, the rate at which the return coil output decays is dependent upon, and indicative of, the composition of the specimen.

By employing an excitation field that has a narrow frequency band, only a relatively narrow band within a nuclear species will be excited. As a result, the transverse magnetic component and, hence, return coil output, will exhibit a relatively narrow frequency band indicative of that band of the nuclear species. On the other hand, if the excitation field has a broad frequency band, the return coil output may include components associated with the transverse magnetic components of a greater variety of frequencies. A Fourier analysis of the output allows the different frequencies, which can be indicative of different chemical or biological environments, to be distinguished.

In the arrangement described above, the contribution of particular spins to the return coil output is not dependent upon their location within the specimen. As a result, while the frequency and decay of the output can be used to identify components of the specimen, the output does not indicate the location of components in the specimen.

To produce such a spatial image of the specimen, gradients are established in the polarizing field. The direction of the polarizing field remains the same, but its strength varies along the x, y, and z axes oriented with respect to the specimen. By varying the strength of the polarizing field linearly along the x-axis, the Larmor frequency of a particular nuclear species will also vary linearly as a function of its position along the x-axis. Similarly, with magnetic field gradients established along the y-axis and z-axis, the Larmor frequency of a particular species will vary linearly as a function of its position along these axes.

As noted above, by performing a Fourier analysis of the return coil's output, the frequency components of the output can be separated. With a narrow band excitation field applied to excite a select nuclear species, the position of a spin relative to the xyz coordinate system can then be determined by assessing the difference between the coil output frequency and the Larmor frequency for that species. Thus, the MRI system can be constructed to analyze frequency at a given point in time to determine the location of spins relative to the magnetic field gradients and to analyze the decay in frequency to determine the composition of the specimen at a particular point.

The generation and sensing of the fields required for proper operation of an MRI system is achieved in response to the sequential operation of, for example, one or more main polarizing field coils, polarizing gradient field coils, rf excitation field coils, and return field coils. Commonly, the same coil arrangement is used to generate the excitation field and sense the return field. A variety of different sequences have been developed to tailor specific aspects of MRI system operation, as described, for example, in U.S. Pat. No. 4,843,322 (Glover); U.S. Pat. No. 4,868,501 (Conolly); and U.S. Pat. No. 4,901,020 (Ladebeck et al.).

One application of conventional MRI systems is in the production of angiograms, or blood vessel images. Various different pulse sequences and processing techniques have been developed for use in MRI angiography, as described in, for example, U.S. Pat. No. 4,516,582 (Redington); U.S. Pat. No. 4,528,985 (Macovski); U.S. Pat. No. 4,647,857 (Taber); U.S. Pat. No. 4,714,081 (Dumoulin et al.); U.S. Pat. No. 4,777,957 (Wehrli et al.); and U.S. Pat. No. 4,836,209 (Nishimura).

As will be appreciated, blood vessels are readily differentiated from surrounding tissue by the pulsatile flow of blood therethrough. MRI angiography exploits this distinguishing characteristic to generate images of the blood vessels in various ways. For example, if the excitation field is pulsed at systole and diastole, the contribution of blood flow to the return field will differ, while the contribution of static tissue and bone to the return field will be the same. By subtracting one return from the other, the static component cancels, leaving only the contribution from the blood vessel.

Unfortunately, because peripheral nerve does not exhibit the flow-distinctiveness of blood vessels, MRI angiography systems and pulse sequences can not be used to generate suitable images of peripheral nerve. Further, conventional MRI systems and sequences used for general imaging of tissue and bone do not provide acceptable results. Given the poor signal-to-noise (S/N) ratio of the return signals (e.g., on the order of 1x to 1.5x) and the small size of the nerve, the conspicuity of imaged nerves relative to other tissue is collectively rendered so poor as to be diagnostically useless.

One technique proposed for use in enhancing the utility of MRI systems in imaging neural tissue involves the use of pharmaceutical agents to enhance the contrast of neural

tissue relative to surrounding tissue in the images produced. As described in PCT Patent Application No. PCT EP 91/01780 (Filler et al., WO 92/04916), published on Apr. 2, 1992, a two-part contrast agent, such as wheat germ agglutinin or dextrin-magnetite, is injected so that it is subsequently taken up, and transported, by the nerve of interest. The first part of the agent promotes neural uptake, while the second part of the agent has the desired "imageable" property.

The agent is injected into muscle and undergoes axoplasmic flow in the nerve supplying that muscle, tagging the nerve in subsequently generated images of the specimen. If MRI is used, the second part of the agent is selected to have a magnetically active (e.g., ferrite) component. An agent having a high nuclear density can, however, be used to increase the contrast of the nerve upon X-ray or computed tomography (CT) examination, while a radioactive (e.g. positron emitting) element can be used to enhance visibility during positron emission tomography (PET) scanning.

To illustrate the effectiveness of contrast agents in imaging nerve, reference is had to FIGS. 1-5. In that regard, FIG. 1 is a diagram of a transverse section of the upper forearm FA of a rabbit. The forearm includes the triceps muscle TM, ulnar nerve UN, brachial veins BV, median nerve MN, radial nerve RN, humerus H, cephalic vein CV, and biceps muscle BM.

FIGS. 2A and 2B illustrate spin-echo MR images of such a section, using a ferrite contrast agent, produced by a conventional MRI system at six-hour intervals. Although some of the larger structural elements are readily identified, the location of some objects appears skewed. More particularly, the humerus marrow appears shifted relative to the humerus H, as do ligaments L, and fat F between the biceps or triceps. In addition, smaller neural structures are difficult to distinguish.

Several approaches are available, however, to attempt to identify nerves in the images generated. For example, as shown in FIG. 3, if a short tau inversion recovery (STIR) sequence of the type described in Atlas et al., *STIR MR Imaging of the Orbit*, 151 AM. J. ROENTGEN. 1025-1030 (1988) is used, the humerus marrow disappears from the image as does, more importantly, certain ambiguous, apparently non-neural structures adjacent the median nerve MN. Thus, as shown in the enlarged image of the region including the median nerve MN and ulnar nerve UN, provided in FIG. 4, the median nerve MN is visible.

Similarly, even when the contrast agent images of FIGS. 2A and 2B are enlarged to better illustrate the region including the median nerve MN, as shown in FIGS. 5A and 5B, respectively, the nerves are distinguishable to a highly skilled observer. More particularly, transport of the ferrite contrast agent during the six-hour interval between the generation of images 4A and 4B results in a loss of intensity in the MN relative to the non-neural structure adjacent median nerve MN. Given this observation and the STIR-based assessment, the median nerve MN can, thus, be identified.

The use of contrast agents, while promising, does have certain limitations. For example, there is an increasing preference to avoid the use of invasive technologies in medicine whenever possible. Further, contrast agents generally can be used to image only a single nerve or nerve group. Of perhaps greatest importance, the contrast agents employed typically reduce the intensity of the imaged nerve. Since nerves are already difficult to see in current MRI images, the impact of the contrast agent upon the image can

be difficult to interpret, as illustrated by the discussion of FIGS. 2-5 above.

In another application, MRI has been used, without contrast agents, to map non-peripheral, white matter nerve tracts in the brain. The white matter tracts extend through gray matter tissue in the brain and exhibit relatively high anisotropic diffusion. More particularly, given their physical structure (i.e., axonal pathways surrounded by myelin sheaths), water mobility along the white matter tracts is relatively high, while water mobility perpendicular to the tracts is low. The surrounding gray matter does not, however, exhibit this same anisotropy.

A technique for MRI-based mapping of white matter nerve tracts that exploits this characteristic of neural tissue is described in Douek et al., *Myelin Fiber Orientation Color Mapping*, BOOK OF ABSTRACTS, SOCIETY OF MAGNETIC RESONANCE IN MEDICINE, p. 910 (1991). Basically, in addition to the fields and gradients described above, this process involves the use of a pair of field gradient pulses (hereinafter referred to as diffusion gradients), oriented perpendicular and parallel to the white matter tracts to be imaged. The effect of a pulsed gradient is to change the phase of the received signal from all of the spins. For stationary spins the effect of the two diffusion gradients cancels out. In contrast, spins moving from one spatial position to another in the time between the two diffusion gradients experience changes in the frequency and phase of the spin magnetization with the net effect being a reduction in the received signal. The signal reduction is greatest for those spins that diffuse the greatest distance between the two pulsed gradients.

As noted above, given the anisotropic nature of the tracts, water will diffuse freely along a tract, but is restricted in its motion perpendicular to the tract. When the diffusion gradient is aligned with the tract there is thus a greater reduction in signal than when the diffusion gradient is aligned perpendicular to the tract. Because this phenomenon is not exhibited by the surrounding gray matter tissue, the white matter tracts can be identified.

Anisotropic diffusion is also a recognized characteristic of peripheral nerve, as indicated in Moseley et al., *Anisotropy in Diffusion-Weighted MRI*, 19 MAGNETIC RESONANCE ON MEDICINE 321 (1991). The Douek et al. technology, however, does not distinguish peripheral nerve from muscle and other tissue for a number of previously unrecognized reasons. First, while the size and structure of the white matter tracts ensure that the resultant signals will be sufficiently strong for imaging, peripheral nerve is considerably smaller and more difficult to distinguish. Second, unlike the white matter tracts, peripheral nerve is commonly surrounded by muscle and fat, both of which impair the ability of the Douek et al. system to image nerve.

By way of elaboration, given its fibrous structure, muscle also exhibits diffusional anisotropy, as recognized in Moseley et al., *Acute Effects of Exercise on Echo-Planar T₂ and Diffusion-Weighted MRI of Skeletal Muscle in Volunteers*, BOOK OF ABSTRACTS, SOCIETY OF MAGNETIC RESONANCE IN MEDICINE 108 (1991). As a result, the simple anisotropic analysis of Douek et al. is unable to distinguish peripheral nerve and muscle. While fat is isotropic and, therefore, distinguishable from nerve, it also impairs the imaging of peripheral nerves. Specifically, the relative signal strength of fat returns to neural returns is so high as to render peripheral nerves unidentifiable in images produced.

As will be appreciated from the preceding remarks, it would be desirable to develop a method for rapidly and

non-invasively imaging a single peripheral nerve, or an entire neural network, without resort to contrast agents. The images generated should be sufficiently detailed and accurate to allow the location and condition of individual peripheral nerves to be assessed. It would further be desirable to provide a system that processes neural images to enhance the information content of the images, diagnose neural trauma and disorders, and inform and control the administration of treatments and therapy.

SUMMARY OF THE INVENTION

The present disclosure relates to a new method, which quite remarkably, is capable of generating a three dimensional image of an individual patient's nerves and nerve plexuses. The image can be acquired non-invasively and rapidly by a magnetic resonance scanner. These images are acquired in such a way that some embodiments of the invention are able to make all other structures in the body including bone, fat, skin, muscle, blood, and connective tissues tend to disappear so that only the nerve tree remains to be seen. A plurality of the nerves passing through a given imaged region may be observed simultaneously, thus alleviating any ambiguity of nerve identification which might arise were only a single nerve imaged as with some contrast agent techniques.

The invention is based on the discovery of a method of collecting a data set of signal intensities with spatial coordinates which describes the positions of the nerves within any two dimensional cross section of a living mammal or within any three dimensional data acquisition space. There exist a large number of pulse sequences capable of controlling or operating a magnetic resonance imaging apparatus and each of which accomplishes some preferred image optimization. Previously, however, no simple (single) or complex (double or multiple) pulse sequence has been able to increase the relative signal intensity of nerve so that it is brighter than all other tissues in the body or limb cross section. Surprisingly, the inventors have discovered that there are certain novel ways of assembling complex pulse sequences, wherein even though the simple components of the sequence decrease the signal-to-noise ratio of nerve or decrease the signal strength of nerve relative to other tissues, the fully assembled complex sequence actually results in the nerve signal being more intense than any other tissue. In this fashion, the image conspicuity of nerve is greatly increased.

Thus, a first aspect of the present invention provides a method of selectively imaging neural tissue of a subject without requiring use of intraneural contrast agents, the method comprising subjecting part of the subject anatomy to magnetic resonance imaging fields, detecting magnetic resonance and producing an image of neural tissue from said detected resonance so that a nerve, root, or neural tract of interest in said image can be visually differentiated from surrounding structures.

A second aspect of the present invention provides a method of selectively imaging neural tissue of a subject, the method comprising subjecting part of the subject anatomy to magnetic resonance imaging fields adapted to discriminate anisotropy of water diffusion or other special characteristic of neural tissue, detecting magnetic resonance to produce an electronic signal in accordance with said resonance and producing an image of neural tissue from said electronic signal.

The invention also provides an apparatus for selectively imaging neural tissue of a subject without requiring the use of neural contrast agents, the apparatus comprising means

for subjecting part of the subject anatomy to magnetic resonance fields, means for detecting magnetic resonance to produce an electronic signal in accordance with said resonance, and means for producing an image of neural tissue from said electronic signal so that a nerve, root, or neural tract of interest in said image can be visually differentiated from surrounding structures.

The invention also finds expression as an apparatus for imaging neural tissue of a subject, the apparatus comprising means for subjecting part of the subject anatomy to magnetic resonance fields adapted to discriminate anisotropy of water diffusion, means for detecting magnetic resonance to produce an electronic signal in accordance with said resonance and means for producing a selective image of neural tissue of interest from said electronic signal.

BRIEF DESCRIPTION OF THE DRAWINGS

The foregoing aspects and many of the attendant advantages of this invention will become more readily appreciated as the same becomes better understood by reference to the following detailed description, when taken in conjunction with the accompanying drawings, wherein:

FIG. 1 is a diagram of a transverse section of the upper forearm of a rabbit illustrating various neural and non-neural structures;

FIGS. 2A and 2B are images of the upper forearm of a rabbit, of the type depicted in FIG. 1, produced using an MRI system at two spaced-apart times after the forearm was injected with a ferrite contrast agent;

FIG. 3 is another image of the upper forearm of a rabbit produced using an MRI system employing a short tau inversion recovery (STIR) spin-echo sequence;

FIG. 4 is an enlargement of a portion of the image of FIG. 3 associated with a peripheral nerve of interest;

FIGS. 5A and 5B are enlargements of a portion of the images of FIGS. 2A and 2B, respectively, associated with a peripheral nerve of interest;

FIG. 6 is a block diagram of a neurography system, constructed in accordance with this invention, coupled to a plurality of other systems designed to provide information to the neurography system and to implement, for example, neural diagnoses, therapy, surgery, and training;

FIG. 7 is a functional chart of the operation of the neurography system of FIG. 6;

FIG. 8 is an illustration of the various components included in the neurography system of FIG. 6;

FIGS. 9 and 10 are flow charts depicting one way in which the neurography system of FIG. 8 may be used to generate neurograms;

FIGS. 11A through 11F illustrate one sequence of pulses suitable for use in producing diagnostically suitable images from the neurography system of FIG. 6;

FIG. 12 is another image of the upper forearm of a rabbit produced by an embodiment of the neurography system employing fat suppression;

FIGS. 13A and 13B are additional images of the upper forearm of a rabbit produced by an embodiment of the neurography system employing gradients perpendicular and parallel, respectively, to the anisotropic axis of nerve being imaged;

FIGS. 14A through 14D are images of the upper forearm of a rabbit produced employing gradients of 0, 3, 5, and 7 Gauss/centimeter, respectively;

FIGS. 15A through 15C are images producible by the neurography system with zero, perpendicular, and parallel gradients, while FIG. 15D is an image based upon the images of FIGS. 15B and 15C, referred to herein as a subtraction neurogram

FIG. 16 vector length image of the brain produced using the neurography system of FIG. 8;

FIG. 17 is an arctan image of the brain produced using the neurography system of FIG. 8;

FIGS. 18A through 18D are images of a rabbit forearm produced using the neurography system of FIG. 8, and illustrating the influence of the TE sequence upon the images produced;

FIG. 19 illustrates a splint employed in the neurography and medical systems of the present invention;

FIGS. 20, 21, and 22 are illustrations of images of a human sciatic nerve produced using the neurography system of FIG. 8, with FIGS. 20 and 21 illustrating the ability of the system to image nerve fascicles (in two cross-sectional scales) and FIG. 22 illustrating an axial projection of the nerve;

FIG. 23 is a diagram of a cross-section of a vertebra, illustrating the types of structure present in one neurography application; and

FIG. 24 is a schematic illustration of a surgical system constructed in accordance with this invention for use with the neurography system of FIG. 8.

DETAILED DESCRIPTION OF THE PREFERRED EMBODIMENT

Referring now to FIG. 6, a neurography system 10 is shown as one component of a broader medical system 12. Unlike prior art arrangements, system 10 quickly and non-invasively generates accurate images showing the pattern of individual peripheral nerves, or entire nerve trees, without the use of contrast agents. The system is designed to allow such images, hereinafter referred to as neurograms, to be displayed in two-dimensions, illustrating neural cross sections in the specimen under examination, or in three-dimensions. The images may selectively exclude all other structures within the specimen, or may illustrate the physical relationship of other structures relative to the nerves for reference.

1. Medical System Overview

As shown in FIG. 6, the neurography system 10 included in medical system 12 includes four basic components: MRI system 14, processing system 16, input system 18, and output/display system 20. In the preferred arrangement, the MRI system 14 is a conventional MRI system modified for use in collecting image data of a patient P under examination. The processing system 16 responds to operator inputs applied via input system 18 to control MRI system 14 and process its output to display the resultant neurograms at system 20. As will be described in greater detail below, system 16 employs a variety of different imaging protocols, alone or in combination, to ensure that the images produced are of a quality heretofore unachieved.

The medical system 12 includes a number of components that supplement the imaging information produced by system 10 and/or use that information for a variety of purposes. For example, an auxiliary data collection system 22 may be included to collect image information about non-neural structures, such as blood vessels and bone, in the imaged region of patient P. This information can then be used to

suppress and/or enhance the appearance of those structures in the neurograms produced by system 10.

A diagnostic system 24, included in system 12, may be used to analyze the images produced by system 10. Given the high resolution, detail, and accuracy of neurograms produced by system 10, system 24 can be programmed to analyze neural pathway information to detect discontinuities associated with, for example, neural compressions, injuries, and tumors. System 24 provides outputs indicative of the location of discontinuities and may, by consultation with a database of image information associated with clinically assessed abnormalities, provide an indication of the nature and magnitude of an imaged discontinuity. These outputs can be used for diagnosis, or applied as feedback to system 10 to refine a region of interest (ROI) under examination in patient P.

Medical system 12 may also include a therapeutic system 26 and surgical system 28. Systems 26 and 28 employ information about the patient's neural structure from system 10 to assist in the proper administration of a desired therapeutic or surgical operation. For example, the information may be used to guide a robotic stylus to a damaged neural site for treatment or to allow an operation on non-neural structure to be performed without damage to the patient's peripheral nerves. The systems 26 and 28 may operate independent of physician control or may simply provide the physician with real-time feedback concerning the relationship between an operation being performed and the patient's neural structures.

A training and development system 30 is included in the medical system 12 for a variety of different purposes. For example, the training system 30 may be used to demonstrate the anatomy of various neural structures, along with their positional relationship to non-neural patient structures. This information has great educational value given the extremely limited ability of prior art techniques, including direct examination, to provide detailed anatomical information. Training system 30 may also be designed to analyze the effectiveness of neurography system 10 and provide feedback used to control the pulse sequences and other operational parameters of system 10.

As one final component, medical system 12 may include a host processing system 32 in addition to, or in place of, separate processing systems in the other components of system 12. Although not separately shown in FIG. 6, system 32 includes a central processing unit (CPU) coupled to the remainder of system 12 by input/output circuits. Memory is provided to store software instructions, used to control the operation of the CPU and, hence, the various components of system 12, and to store image and other data collected by system 12. The use of a separate host processing system 32 is particularly desirable where various components of system 12 are to be operated in interactive fashion pursuant to a single set of software instructions.

2. The Neurography System

Turning now to a more detailed discussion of neurography system 10, by way of introduction, some of the more important operational features of system 10 are loosely depicted in the chart of FIG. 7. As will be described in greater detail below, system 10 may be constructed to employ one or more of these features to enhance the imaging ability of conventional MRI sufficiently to provide diagnostically and therapeutically useful information.

As shown, the operation of system 10 can be broken down into the broad steps of data collection 34, image processing and analysis 36, image display 38, and control 40. The data collection process 34 involves, for example, spin-echo imag-

ing 42, which may be supplemented by one or more of the following imaging protocols: fat suppression 44, diffusion weighting 46, and "long T2" processing 48, and other protocols including magnetization transfer. Each of these protocols has been found to enhance the quality of images of peripheral nerve sufficiently to provide heretofore unavailable MRI neurograms.

The data collected by process 34 is subjected to image processing and analysis 36, involving two-dimensional and three-dimensional image generation 50. Image generation 50 may be further enhanced by miscellaneous suppression features 52, responsible for reducing the influence of, for example, blood vessels and patient motion, on the images produced. An image subtraction feature 54 may also be employed to remove all non-neural components from the images.

a. Neurography System Construction

Having briefly summarized the operational aspects of neurography system 10, its construction and operation will now be considered in greater detail. In one embodiment, MRI system 14 includes an imager I of the type sold by GE Medical Systems, under the trademark SIGNA (software release 5.2).

In that regard, as shown in FIG. 8, the region R of the patient to be imaged is placed within the bore B of the MRI system imager I. As will be described in greater detail below, the position of region R relative to the imager may be stabilized by a splint 58. Splint 58 limits motion artifact, provides fiducial markers in a secondary frame of reference, and reduces the system's susceptibility to boundary effects that otherwise might degrade fat suppression near the boundary between skin and air.

MRI system 14 includes polarizing field coils 60 and 61 responsible for exposing region R to the desired polarizing field. The polarizing field has a strength of, for example, 1.5 Tesla and is oriented along a z-axis.

A tuned rf excitation coil 62 is also positioned within bore B over the region R under investigation. Coil 62 is provided with a pulsed rf input, in a manner described below, to generate the field responsible for excitation of nuclear spins in region R. Coil 62 is also responsible for detecting the rf return, or echo, fields generated by the spins, although separate transmit and receive coils may alternatively be used.

The excitation coil 62 may be, for example, a solenoid or surface coil, configured and dimensioned to fit closely over the region R to be imaged (e.g., the patient's arm, leg, shoulder, chest, pelvis, head, neck or back). In a preferred arrangement, however, a phased array coil system is employed to increase the signal-to-noise ratio of the returns, thereby providing an improvement in the spatial resolution of system 14 and allowing information to be retrieved from signals that would otherwise have been too weak to form useful images. For example, where peripheral nerve having a thickness on the order of 1-2 mm is to be sharply resolved, each array includes, for example, 4-6 individual coils, arranged in transverse and longitudinal pairs or linear paired arrays.

Three pairs of gradient coils 64 and 66 are also positioned within the bore B of the imager. These coils superimpose a locational gradient of roughly one Gauss per centimeter upon the polarizing field over the sample region R along each of the x, y, and z-axes. For the sake of simplicity, however, only the z-gradient coils 64 and 66 are shown in FIG. 8.

In the preferred arrangement, the same coil pairs 64 and 66 are used to produce diffusional gradients along the

desired axes, as well as the requisite locational gradients. Alternatively, one or more separate diffusional gradient coil pairs 68 and 70 may be provided within the imager bore B. If the separate coil pair 68 and 70 is mounted on a movable track, substantially any desired diffusional gradient orientation can be achieved. The diffusional gradient is relatively strong compared to the locational gradients, e.g., ranging up to 10 Gauss/centimeter or higher.

A computer 72 and front-end circuit 74 form the processing system 16, input system 18, and output/display system 20 of neurography system 10 shown in FIG. 6. Computer 72 and circuit 74 cooperatively control and synchronize the operation of MRI system 14, as well as process and display the acquired data.

The computer 72 is, for example, an IBM-compatible personal computer including a 486 processor, VGA monitor, and keyboard. An interface bus 76, included in circuit 74, couples computer 72 to the other components of circuit 74.

A gradient pulse generator 78 included in circuit 74 produces generally rectangular output pulses used to establish the desired gradients in the polarizing field. The output of generator 78 is applied to x-, y, and z-axis gradient field amplifiers 80, although only the z-axis amplifier 80 is shown in FIG. 8. As will be appreciated, if separate coils 68 and 70 are employed to establish the diffusional gradients, the output of generator 78 must be applied to those coils via separate amplifiers 82.

Circuit 74 also includes an rf pulse generator 84, which produces rf signal pulses used in the establishment of the excitation field. In the preferred arrangement, the pulse generator produces an rf output suitable for use in proton MRI, although frequencies specific to other MRI susceptible nuclei, such as, ¹⁹fluorine, ¹³carbon, ³¹phosphorus, deuterium, or ²³sodium, may be used. The output of generator 84 is amplified by a high-power rf amplifier 86 before being selectively applied to the excitation coil 62 by a duplexer 88. The duplexer 88 is also controlled to selectively steer the low level MR returns received by the excitation coil 62 to a preamplifier 90.

A mixer 92 transforms the high frequency output of preamplifier 90 to a low frequency signal by mixing the amplified MR returns with signals from a digitally controlled rf oscillator 94, which also provides inputs to generator 84. The analog output of mixer 92 is input to a low pass filter 96 before finally being converted to a digital form by an analog-to-digital converter 98. The computer 72 processes the resultant digital inputs, which represent the response of the spins to the applied fields, to generate the desired neurograms.

b. Neurography System Operation

Having reviewed the basic construction of the neurography system 10, its operation to generate the desired two- or three-dimensional neurograms will now be considered. To that end, FIGS. 9 and 10 depict the general sequence of steps performed by system 10 in the production of neurograms. These neurograms exhibit a high nerve conspicuity, which for the purpose of the ensuing discussion will be understood to refer to the contrast (in, for example, intensity or color) between the nerve and the image background. The methods described below may be used to produce neurographic images of substantially any region of the body, including the brain, for example, central nervous system (CNS) neurograms.

As indicated at block 100, the operation of the system is first initialized to establish certain parameters of the system's operation. In that regard, the operator may input desired parameters via computer 72 in response to queries

generated at start up. Because most aspects of the system's operation are controlled by software resident in the memory of computer 72, default initialization parameters may also be accessed.

Although the particular parameters to be initialized may vary at the user's discretion, examples include the type of images to be generated (i.e., two-dimensional cross sections or three-dimensional projections), field of view (FOV), thickness of each slice imaged, pulse repetition rate (TR), number of phase encoding steps, the existence of a known axis of diffusional anisotropy, and the strengths and orientations of the diffusional gradients to be used. By way of example, the operator may select a two-dimensional image, a FOV of four cm by four cm, a TR of 1.5 seconds, and 256 phase encoding steps. A discussion of anisotropic axis identification is provided below.

Once initialization has been completed, a series of steps, corresponding to the data collection process 34 discussed in connection with FIG. 7, are performed. This process generally involves the control of pulse sequences used in connection with front end circuit 74. As will be described in greater detail below, different sets of pulse sequences and combinations of pulse sequences have been devised to unambiguously distinguish small peripheral nerves from neighboring structures of similar shape and location, including the combination of certain existing sequences into new groupings for use in new situations and the design of new sequences that incorporate optimized features for the purpose of neurographic imaging. For illustrative purposes, a graphic illustration of one example of a suitable pulse sequence is provided in FIGS. 11A through 11F.

i. Fat Suppression

As indicated in block 102 of FIG. 9, a first, optional, step performed in the image generation process is fat suppression. Although fat represents a known source of interference in MRI images of bone and tissue, it was not previously recognized as an impediment to effective neural imaging due to the broader perception that neural MR signals were inadequate for imaging regardless of background composition. The value of fat suppression was discovered during the development of the present invention by the fortuitous use of a main field magnet designed for spectroscopy as part of an imaging system.

In that regard, in MR spectroscopy, a relatively strong magnetic field is employed to increase the separation in frequency between signals arising from different chemical species of the same nucleus, thereby allowing these components to be more easily distinguished. MRI also uses a frequency distribution (created by applying a field gradient) over a sample to locate spins and create an image. The signals from fat and water are at slightly different frequencies and therefore appear shifted relative to each other in an image.

The fat/water shift is relatively small when a low field, clinical MRI system is used. Fortuitously, a much stronger spectroscopic field magnet was used during initial efforts at imaging nerve, introducing a much greater displacement of fat in the image produced. With the high intensity fat signal shifted away from the nerve, an enhancement of the nerve's conspicuity was observed. The recognition of this enhancement led to the realization that effective neural imaging could, in fact, be achieved through the inclusion of fat suppression in system 14.

Fat suppression apparently enhances the use of conventional MRI systems for neurography in several ways. First, the removal of extraneous components reduces the number of imaged structures to be distinguished. Second, in a fat

suppressed image a peripheral nerve exhibits a relatively high intensity and will stand out sharply against the low intensity space left behind by the suppressed fat. As will be described in greater detail below, fat suppression also synergistically increases the apparent magnitude of diffusion anisotropy and magnetization transfer effect.

One suitable fat suppression technique involves the use of a chemical shift selective (CHESS) pulse sequence, described in detail, for example, in Haase et al. *NMR Chemical Shift Selective Imaging*, 30 PHYS. MED. BIOL. 341-344 (1985).

As shown in FIG. 11A, CHESS involves the application of a sequence of narrow band rf pulses A, B and C to the excitation coil 62 to selectively excite the nuclear spins of fat molecules within the region R of the patient being imaged. By way of example, three millisecond Gaussian pulses having a minus three dB bandwidth of 600 Hertz may be employed. A sequence of gradient pulses a, b, and c is then applied to the three sets of gradient coils 64 and 66 to dephase the excited spins, thereby minimizing the contribution of the fat signals to the final image. The gradient pulses a, b, and c applied to the orthogonal gradient coil pairs produce, for example, gradients of five Gauss per centimeter for three milliseconds along the x, y, and z-axis, respectively.

FIG. 12 illustrates the effect of fat suppression on neurograms produced with the MRI system 14. The image provided in FIG. 12 is of the forearm of a rabbit and corresponds to the images of FIGS. 1-5 described above. The darker portions of the image represent greater image intensity. As shown in FIG. 12, the ulnar nerve UN and median nerve MN are readily identified.

As an alternative to the use of CHESS for fat suppression, the desired suppression may be effected by selective water stimulation. Other suitable alternatives include the Dixon technique for fat suppression described in, for example, Dixon et al., *Simple Proton Spectroscopic Imaging*, 153 RADIOLOGY 189-194 (1984) and also STIR (short tau inversion recovery) described in *Improved Fat Suppression in STIR MR Imaging: Selecting Inversion Time through Spectral Display*, 178 RADIOLOGY 885-887 (1991).

Although in the preferred embodiment fat suppression is combined with other techniques such as diffusional weighting and long T_2 processing, fat suppression by itself enhances conventional MRI processing sufficiently to generate clinically useful neurograms. Similarly, as will be described in greater detail below, other techniques employed by system 10 can be used without fat suppression to generate suitable neurograms.

ii. Spin-Echo Sequence (Without Diffusional Weighting)

Having discussed the optional introductory portion of the illustrative pulse sequence depicted in FIG. 11, the next phase of the neurography system's operation will now be considered.

In that regard, an rf excitation pulse D, shown in FIG. 11A, is applied to coil 62 to tilt the net magnetic moment of the spins by ninety degrees relative to the polarizing field, into the transverse plane. The resultant maximum transverse magnetization then decays to zero as the spins dephase. A second pulse E, having twice the intensity of pulse D, is applied to coil 62 after a delay of one-half the return or echo time (TE). This pulse rotates the spins a further 180 degrees and causes a spin-echo to form as the spins rephase. The spin echo has a maximum amplitude after a further delay of TE/2. A spin-echo signal F is, thus, generated in coil 62 at time TE in response to the combined influence of excitation pulse D and refocusing pulse E. These steps are depicted in blocks 104, 106, and 108 of FIG. 9.

At the same time, the imaging gradients are produced by the orthogonal coil pairs 64 and 66 to encode the echo signal F in the usual manner, allowing an MR image to be constructed, as indicated in block 110. With the sample oriented along the z-axis, the "slice select" pulses d, d', and e shown in FIG. 11C are applied to the z-axis coil pair 64 and 66, to excite and refocus the z-axis slice of interest. The "readout gradient" pulses f and f', shown in FIG. 11D, are applied to, for example, the x-axis coil pair 64-66 to achieve the desired output that is to be Fourier transformed. The "phase encoding" pulses g and g', shown in FIG. 11E, are applied to the y-axis coil pair 64 and 66, to control the number of echoes (e.g., 256) to be received. The sequence may be used to generate images from contiguous slices or regions of the patient.

As will be appreciated, if the operator indicates (at block 100) that diffusional weighting is not required for the generation of a particular image by neurography system 10, the pulses shown in FIGS. 11A-11E define substantially the entire spin-echo sequence. Even if diffusional weighting is to be employed, in the preferred embodiment an initial image is generated using only fat suppression for enhancement and, as a result, diffusional weighting is not used during the first performance of the spin-echo sequence (blocks 104-110) for a particular slice.

Although spin-echo imaging is employed in the preceding embodiment of neurography system 10, other techniques can be employed. Suitable alternative techniques include, for example, stimulated echo imaging and gradient-recalled echo imaging, e.g., echo planar imaging (EPI). Such alternative techniques are described in Parikh, *MAGNETIC RESONANCE IMAGING TECHNIQUES* (1992).

iii. Echo Processing

In the imaging sequence depicted in FIG. 11, a series of echo signals F are acquired to create a two-dimensional image. For example, at block 112 in FIG. 9, 256 echoes with 256 different phase encoding gradient amplitudes are used to construct a 256-by-256 pixel image. The data set is then enlarged at block 114 by zero filling to produce a 1024-by-1024 matrix of data. As a result, the apparent resolution of the final image is increased, making the image clearer.

Next, the enlarged data set is processed using a 2D Gaussian filter at block 116. The filter smoothes the image by attenuating the high frequency components in the image and, thus, clarifies the delineation of small details without altering the relative average pixel intensities over a region of interest. At block 118, the two-dimensional matrix of data then undergoes a two-dimensional Fourier transform, which yields an image to be stored. If desired, the image may also be displayed on the computer monitor, although in the preferred arrangement this image is but one component used in a more extensive analysis performed to generate a select, enhanced image.

Once an initial image has been generated, the analysis of the image is initiated, as shown in FIG. 10. At block 122, one or more regions of interest (ROI) within the image can be identified. Each ROI may be a single pixel or voxel, or a larger region. ROI selection can be performed manually using, for example, a keyboard or mouse to move a cursor over the ROI on the displayed image. Alternatively, ROI selection may be accomplished automatically via a sequential selection of all pixels or via an external input regarding a particular region from, for example, diagnostic system 24.

Next, the average image or pixel intensity within each ROI is computed at block 124. This average image intensity S can be represented by the following expression:

$$S = A_0 [\exp(-TE/T_2)] [\exp(-bD)] \quad (1)$$

where A_0 is the absolute signal intensity for a particular pixel and b is the gradient factor, determined in accordance with the expression:

$$b = \gamma^2 (G_z^2) (\delta^2) (\Delta - \delta/3) \quad (2)$$

where γ is the gyromagnetic ratio, G_z is the polarizing field strength, δ is the length of a diffusional weighting gradient pulse, and Δ is the interval between diffusional weighting gradient pulses. As will be appreciated, in the first iteration before diffusional weighting is employed, the final term of equation (1) is, thus, unity.

To make use of the expressions in equations (1) and (2), the preceding data acquisition process is repeated for different values of echo time TE. On the other hand, if diffusional weighting is employed, as described in greater detail below, the data acquisition process is repeated for different gradient strengths (controlled by adjusting gradient magnitude and/or duration) or gradient orientations. For example, TEs of 30, 60, 90, and 110 milliseconds, or gradient magnitudes of 0, 3, 5, and 7 Gauss/centimeter, may be employed. The image intensity S for a particular pixel of these multiple images of the same transverse slice for particular values of TE (or b , if diffusional weighting is employed) is available and a linear regression analysis of the logarithmic relationship is performed at block 126.

Finally, the value of the apparent T_2 relaxation time (or the apparent diffusion coefficient D , if diffusional weighting is employed) is computed for a particular ROI at block 128. These computations provide quantitative assessments of the various ROI in the image that are useful in subsequent image processing by other components of the medical system 12.

iv. Gradient Orientation for Diffusion Weighting

In the preferred arrangement, after the initial fat suppressed image has been collected and its ROI characterized, a diffusional weighting analysis is initiated to further enhance the neurograms generated by evaluating the diffusional anisotropy exhibited by nerve and other tissue. The first aspect of this analysis is the selection of the diffusional gradients to be used.

By way of introduction, in one currently preferred embodiment, the analysis involves the application of pulsed magnetic field gradients to the polarizing field in two or more directions to produce images in which the peripheral nerve is enhanced or suppressed, depending upon the "diffusion weighting" resulting from the particular pulsed gradient axis chosen. Discrimination of water diffusion anisotropy is then achieved by subtracting the suppressed image from the enhanced image, in the manner described in greater detail below, producing an image depicting only the peripheral nerve.

Most preferably, the magnetic field gradients are applied in mutually substantially orthogonal directions. For example, with gradients approximately perpendicular and parallel to the axis of the peripheral nerve at the particular point being imaged, the parallel gradient image can be subtracted from the perpendicular gradient image to produce the desired "nerve only" image.

As will be appreciated, if the axis of the nerve is generally known to the operator and its relationship to the referential frame of the MRI system 14 has been indicated at initialization block 100, the direction of the desired orthogonal diffusional weighting gradients can be readily determined. On the other hand, if the axis of the peripheral nerve is not known, or if many nerves having different axes are being imaged, the neurography system 10 must employ a system of gradient orientations suitable for imaging nerve having substantially any axial alignment. For example, as will be

described in greater detail below, a full three-dimensional vector analysis can be used to characterize the diffusion coefficient and provide a nerve image by construction based upon a fixed arrangement of diffusion weighting gradients.

In anatomical regions, such as the upper arm or wrist, it is also possible to achieve adequate enhanced isolation of the nerve image by applying only a single diffusion gradient perpendicular to the axis of the nerve at the site of interest. As a result, no subtraction need be carried out to produce the neurogram. The fat suppressed, orthogonally diffusion weighted image can either be processed directly, or it can be subject to threshold processing to remove signals of lower intensity associated with non-neural tissue, or nerves with different axes and directions of travel at the imaging location.

As will be appreciated, for quicker and more efficient data collection and processing, the establishment of diffusion gradients in the polarizing field should be responsive to the particular one of the foregoing scenarios that applies to the imaging problem at hand. Depending upon the inputs provided at block 100, the system may have been advised that (a) only one gradient of known orientation is required, (b) two orthogonal gradients of known orientation are required, or (c) two or more gradients of unknown orientation are required.

As indicated in block 130 of FIG. 10, upon completion of the analysis of an image, the system considers whether all of the desired diffusional gradients have been applied to the polarizing field during subsequent data acquisition by, for example, spin-echo processing, or fast spin-echo processing. Because no diffusional gradient was used in the initial fat suppression processing, the answer is initially NO and operation proceeds to block 132.

There, the computer determines whether the operator initially indicated that the axis of diffusional anisotropy is known. If the axis is known, a perpendicular diffusional gradient is employed, as indicated at block 134. Then, as indicated at block 136, a diffusion-weighted spin-echo sequence is performed (modified by the inclusion of the diffusional gradient in the manner described in greater detail below) and image generated, pursuant to blocks 102-122, before quantification of the image data occurs at blocks 124-128 to compute D or T_2 . If the operator indicated at initialization that orthogonal diffusion gradients are required for the particular imaging problem at hand, this process is then repeated at blocks 138 and 140 for a parallel diffusional gradient.

If the inquiry performed at block 132 determines that the axis of diffusional anisotropy is unknown, operation proceeds to block 142. There an initial diffusional gradient is arbitrarily selected, to be followed by a sequence of alternative gradients selected for use by the operator when the anisotropic axis is unknown.

At block 144, using the initial diffusional gradient, a spin-echo sequence is performed (modified by the inclusion of the diffusional gradient in the manner described in greater detail below) and image generated, pursuant to blocks 102-122, before quantification of the imaged data occurs at blocks 124-128. Then, at block 146, a test is performed to determine whether the desired number of different diffusional gradients (e.g., three gradients, along the x-, y-, and z-axes) have been used. If not, the next diffusional gradient is selected at block 148 and the spin-echo sequence, imaging and processing operations are performed, as indicated at block 144. This process is then repeated until the desired number of alternative diffusional gradients have been employed.

As will be appreciated, additional gradient coils may be provided where gradients are desired along axes other than those provided by the locational gradient coils. To that end, diffusional gradient coils may be mounted on a magnetically compatible, adjustable track within the bore of the imager to allow gradients to be repositioned and applied over a substantially continuous range of orientations. Similarly, the region to be imaged may be movably supported relative to a fixed set of gradient coils to introduce the desired variability in gradient direction. As another option, a plurality of different gradient coils may be employed and activated in various combinations to effect the desired gradient variations. Alternatively, the results obtained from a limited number of gradient directions can be processed using a vector analysis to estimate the results obtainable with a gradients other than those directly available, as described in greater detail below.

v. Spin-Echo Sequence For Diffusional Weighting

As noted briefly above, for each of the different diffusional gradients employed, the spin-echo sequence is repeated, followed by the generation of image data and the processing of that data to, for example, quantify the relaxation time T_2 or diffusion coefficient D . In the preferred arrangement, the use of diffusion gradients influences a number of aspects of the spin-echo sequence.

As shown in FIG. 11F, two pulses h and h' , applied to the desired pair of gradient coils are used to establish a particular diffusional gradient in the polarizing field. For an echo time (TE) of 50 milliseconds, the duration (δ) of each pulse is, for example, 10 milliseconds and their separation (Δ) is 20 milliseconds. In the presence of the diffusional gradient, the echo signal F , and therefore the pixel or voxel intensity in the image ultimately produced, is made sensitive to the spatial diffusion of water molecules in the imaged region R .

In that regard, as indicated above, with the diffusional gradient oriented substantially perpendicular to the diffusionally anisotropic nerve, the nerve image is enhanced and generally exhibits the highest intensity of various features imaged. This phenomena is depicted in FIG. 13A, which is an image of the forearm of a rabbit, corresponding to the diagram provided in FIG. 1. The ulnar nerve UN and median nerve MN are both relatively dark (high intensity) and are easily seen. Alternatively, with the diffusional gradient oriented substantially parallel to the diffusionally anisotropic nerve, the nerve image is suppressed and generally exhibits a lower intensity than other features imaged, as illustrated in FIG. 13B. These images can be combined, via a subtraction process described in greater detail below, to produce an image of the nerve isolated from all other structure.

To reduce the effect of cross-terms between the imaging gradients and the diffusion weighting gradients, the spin-echo sequence illustrated in FIG. 11 is a modified version of conventional sequences. More particularly, the readout gradient rephasing pulse f shown in FIG. 11D, is placed directly before the acquisition of echo F in FIG. 11A, instead of after the slice-selective excitation pulse d , shown in FIG. 11C. However, a consequence of this change was the appearance of artifacts in the non-diffusion-weighted images due to an unwanted echo, presumably formed from imperfections in the slice-selection pulses d , d' , and e , shown in FIG. 11C. To overcome this problem, a second modification of the pulse sequence was made. Specifically, the phase-encoding gradient was split into two sections g and g' , and two or four transients (depending upon S/N) were acquired with phase cycling. As a result, the remaining cross terms contribute less than three percent to the diffusion weighting factor.

Although fat suppression is not required to take advantage of the image enhancements available through diffusional

weighting gradients, in the preferred arrangement, the fat suppression sequence shown in FIGS. 11A and 11B is employed prior to the initiation of the diffusion-weighted spin-echo sequence. As will be described in greater detail below, the combination of these techniques generally provides an image quality that exceeds that available from either technique individually.

The echo F produced using the diffusion weighted pulse echo sequence is processed in the manner described above in connection with blocks 112 through 128 of FIGS. 9 and 10. With diffusion weighting, the computation of the diffusional coefficient D at block 128 is preferably based upon the analysis of data collected for different gradient magnitudes. For example, the computation may be based upon gradients of 0, 3, 5, and 7 Gauss/centimeter, resulting in the production of image data as represented in FIGS. 14A through 14D, respectively. While fat, bone, marrow, skin and vessels are generally absent even at the lower gradients, muscle and ligaments drop out at the higher gradients. As suggested previously, the increasingly stronger gradients may be achieved by increasing gradient duration, rather than magnitude. Alternatively, the iterative data collection process may be performed using different gradient directions.

vi. Image Selection/Production

Once computer 72 determines, at block 130, that images have been collected for all of the desired diffusional gradients, operation proceeds to block 150. If the axis of anisotropy is unknown, the various diffusional coefficients D computed for each ROI using different gradient orientations are compared at block 150 to identify the maximum and minimum values. These coefficients provide a measure, associated with each pixel or voxel, of the magnitude of diffusional anisotropy at that point, while the anisotropic direction is indicated by the gradient orientation.

(a) Subtraction Neurography

In the preferred arrangement, the images associated with the maximum and minimum values of the diffusional coefficients for a particular ROI are then used in a subtraction process, as indicated at block 152. The image associated with the larger coefficient is produced by a gradient that is more nearly perpendicular to the neural axis, enhancing the nerve image, while the image associated with the smaller coefficient is produced by a gradient that is more nearly parallel to the axis, selectively destroying the nerve signal. When these two penultimate images are then mathematically (or photographically or optically) subtracted from one another, a subtraction neurogram is produced.

By way of illustration, FIG. 15A is an image produced without diffusion weighting. FIGS. 15B and 15C then illustrate images produced using parallel and perpendicular gradients, respectively. Finally, the subtraction neurogram produced when the image of FIG. 15C is subtracted from that of FIG. 15B is shown in FIG. 15D.

This "ideal" neurogram is somewhat analogous to a subtraction angiogram (an image showing only blood vessels), but sharply highlights a nerve rather than a vessel. Such an image is particularly useful for confirming the identification of nerves in a given imaging plane or space as well as for locating nerve injuries and nerve compressions. Despite the well known existence of angiograms showing the entire vascular pattern in an anatomic region, and despite the existence of MRI techniques that could have been applied to the problem of neural imaging techniques, and despite the great need for the visualization of nerves, particularly, in isolation, there has not previously been any way of creating such neurograms.

Although image subtraction is employed in the preferred arrangement, it is not necessary. For example, in some

applications of known anisotropy, subtraction is unnecessary and can be foregone in favor of a threshold analysis. Also, the subtraction process can be further supplemented, if desired. For example, the output of the subtraction process can be divided by the signal information from a fat suppressed, T₂-weighted spin echo sequence (e.g. using the aforementioned CHESSE technique).

One potential problem to be addressed by the use of the subtraction process is image registration. As will be appreciated, provided that non-neural tissue is identically located in both images subjected to the subtraction process, the non-neural component will cancel out of the resultant image. On the other hand, if some shift or other discrepancy in the apparent position of non-neural tissue is introduced into an image due, for example, to movement of the subject, cancellation may not occur and the nerve may actually be more difficult to identify in the resultant image.

In one embodiment, acceptable image registration is evaluated prior to initiation of the subtraction process. More particularly, the intensities of pixels in one image are compared to the intensities of corresponding pixels in the second image. Pixels of neural tissue are disqualified on the basis of their high diffusional anisotropy, assessed via their diffusion coefficients. Unless the intensities of the remaining, non-neural pixels fall within a certain range of each other, indicating acceptable image registration, subtraction will be inhibited.

(b) Vector Processing and Three-Dimensional Image Generation

Up to this point, the output produced is generally in the form of a single two-dimensional image, or a series of two-dimensional images that can be related to form a three-dimensional image. In a simple form of three-dimensional image generation, described in greater detail below, the high S/N ratio of the two-dimensional neurograms produced by system 14 readily allows the imaged nerve cross-sections to be identified and then linked together to form a three-dimensional projection of the neural structure.

As will be appreciated, however, depending upon the neural pattern involved and the spatial resolution required, this simplified approach may introduce undesired discontinuities into the three-dimensional projection. A more sophisticated processing scheme employs information about the anisotropic direction of the nerve in each two-dimensional image to further enhance the accuracy of three-dimensional image projections. The availability of information regarding anisotropic direction is also useful in establishing the optimal directions for the gradients used in the diffusional weighting analysis described above to produce a two-dimensional image.

In that regard, the anisotropic axis of the peripheral nerve being imaged is sometimes known to the operator, allowing the operator to input the directional information at block 100 and select the best diffusional gradients for imaging. More commonly, however, nerves and CNS neural tracts follow relatively complex paths and the direction in which the diffusion anisotropy coefficient of the nerve or tract is greatest gradually shifts from one plane or axis to another as the nerve or tract curves or turns. As a result, one or two arbitrarily oriented, standard gradients may be inadequate to provide the desired images.

Changes in neural direction can be monitored by moving the patient relative to a fixed set of gradient coils or employing movable diffusional gradient coils mounted, on a track with a non-magnetic drive system, within the bore of the imager to adjustably control the orientation of the diffusional gradients applied to the region of interest. By

monitoring changes in the ratio of D_{pl}/D_{pr} obtained for a given pixel using alternative gradient alignments, or for sequential pixels using the same gradient alignments, changes in neural direction can be estimated and suitable gradient directions selected. Alternatively, gradient coils oriented in three planes can be simultaneously activated in various combinations to achieve the effect of an infinite variety of differently oriented gradients.

One advantage of attempting to track changes in neural direction is that parallel and perpendicular gradient information can then be collected and used to produce a subtraction neurogram of the type described above. If, however, the optimal gradient directions for a given pixel are determined using feedback from images generated with repetitively adjusted gradients, processing speed may be significantly impaired.

In many cases the well known anatomy of a nerve will permit the use of a particular axis orientation in advance. Initial imaging information will provide a description of the gross course of the nerve. A subsequent "informed" approximation can optimize the orientation in each slice. This can be useful to insure excellent homogeneity of nerve image intensity or to measure the coefficient of anisotropy along the course of the nerve.

As a preferred alternative, requiring less mechanical complexity and faster processing speed, a technique has been developed for observing diffusional anisotropy, independent of its degree of alignment with any individual gradient axes. This process involves the combination of information from anisotropy measurements obtained along three standard orthogonal axes or using information from multiple fixed axes. For example, in the preferred embodiment, a vector analysis is used to produce interpolated images and directional information from the three orthogonal diffusion-weighted images described above.

In that regard, image information is collected from, for example, four "multi-slice" sets using a zero diffusion gradient B₀ and diffusion gradients B_x, B_y, B_z in the x-, y-, and z-orthogonal directions, respectively. For each pixel in the image to be produced, information concerning the corresponding pixels in the four diffusion gradients images is combined to produce a diffusion vector, representative of water molecule movement along the nerve fiber in either direction. This vector has a magnitude representative of the image intensity of the pixel and a direction representative of an "effective" diffusion gradient associated with the pixel.

More particularly, the image intensity S_n of a given pixel in the new image is calculated using the following vector equation:

$$S_n = \text{vector length} = (S_x^2 + S_y^2 + S_z^2 + S_0^2)^{1/2} \quad (3)$$

where S_x, S_y, and S_z are the image intensities of the corresponding pixels in the images produced by the B_x, B_y, and B_z gradients. S₀ is the image intensity of the corresponding pixel in the image produced by the B₀ gradient and is included in equation (3) to normalize the resultant image intensity S_n. The direction of the effective gradient associated with this pixel image includes components θ_{xy}, θ_{xz}, and θ_{yz}, computed in the following manner:

$$\theta_{xy} = \text{diffusion vector angle between } B_x \text{ and } B_y = \arctan(S_y/S_x) \quad (4)$$

$$\theta_{xz} = \text{diffusion vector angle between } B_x \text{ and } B_z = \arctan(S_z/S_x) \quad (5)$$

$$\theta_{yz} = \text{diffusion vector angle between } B_y \text{ and } B_z = \arctan(S_z/S_y) \quad (6)$$

The parameters computed in equations (3), (4), (5), and (6) can be used to generate images in a variety of different